CERN-SPSC-2022-032 / SPSC-I-258

7 November 2022

BDF/SHiP at the ECN3 high-intensity beam facility

Letter of Intent

[1]BDF Working Group, SHiP Collaboration

Abstract

The BDF/SHiP collaboration has proposed a general-purpose intensity-frontier experimental facility operating in beam-dump mode at the CERN SPS accelerator to search for feebly interacting GeV-scale particles and to perform measurements in neutrino physics. BDF/SHiP complements the world-wide program of New Physics searches by exploring a large region of parameter space which cannot be addressed by other experiments, and which reaches several orders of magnitude below existing bounds. The SHiP detector is sensitive both to decay and scattering signatures of models with heavy neutral leptons, dark photons, dark scalars, axion-like particles, light dark matter and other feebly interacting particles. In neutrino physics, BDF/SHiP can perform unprecedented measurements with tau neutrinos and neutrino-induced charm production. Following the Technical Proposal submitted in 2015, the subsequent three-year Comprehensive Design Study (CDS), and the recent study of BDF/SHiP in existing beam facilities around the SPS, this paper restates the motivation and reports on the implementation and physics performance of BDF/SHiP in the SPS ECN3 high-intensity beam facility.

Keywords: Beam Dump Facility, BDF, SHiP, SPS, ECN3

Contacts: Andrey.Golutvin@cern.ch, Richard.Jacobsson@cern.ch, Matthew.Fraser@cern.ch

[1]Complete author lists at the end

1 Introduction

BDF/SHiP is a state-of-the-art experimental setup designed to perform a generic and exhaustive search for feebly interacting particles (FIPs) in a region of mass and coupling that is only accessible with a dedicated beam-dump configuration. The proposal aims at taking full advantage of the opportunities offered by the available but unused 4×10^{19} protons at 400 GeV at the CERN SPS accelerator. The physics programme includes a search for New Physics through both decay and scattering signatures. The details of the development of the project starting from the proposal in 2013 can be found in Ref. [1-14]. The reference section at the end of this LoI also includes the complete lists of reports submitted on the facility [15-40] and detector developments [41-76], physics studies [77-87], development in theory [88-107], and PhD theses [108-127] in the context of BDF/SHiP.

The Deliberation Document of the 2020 Update of the European Strategy for Particle Physics [128] (ESPPU2020) recognised the BDF/SHiP proposal as one of the front-runners among the new facilities [129-131] investigated within the PBC studies. To respond to the financial constraints that prevented considering the project for approval in 2020, a continued programme of R&D was launched as part of the CERN Medium Term Plan 2021-2025 [132] with the objective for the BDF Working Group [133] to review the design of the facility, aiming for an alternative implementation in an existing beam facility around the SPS in order to significantly reduce the cost with respect to the initial proposal while preserving the original physics scope and reach of the facility.

This effort has been accompanied by a revision of the detector layout by the SHiP collaboration with the goal of reducing the size and the overall space required, in order to fit in existing underground areas. A dedicated collaboration agreement between the SHiP institutes and CERN has been established through a Memorandum of Understanding [134] in 2021 to ensure a coherent optimisation effort between the facility and the experiment. **The result of this location and layout optimisation study [1] identified ECN3 as the most suitable and cost-effective option. The decision of the CERN management to review the post-LS3[2] physics programme in ECN3 [135,136] prompted the BDF/SHiP collaboration to pursue the studies of the facility and of the SHiP detector aimed at ECN3, and to verify, by full simulation, the physics performance. The use of ECN3 for BDF/SHiP entails a major cost-saving when compared to the original proposal. This document reports on the results of the studies performed for ECN3 and formally express intent to construct BDF/SHiP in ECN3.**

2 Physics motivation

The triumph of the Standard Model is still far from closing the quest for new particles. Several well-established observational phenomena — neutrino masses and oscillations, dark matter, and the baryon asymmetry of the Universe — cannot be explained with known particles alone and clearly indicate that New Physics exists. This New Physics might also help us to understand peculiar properties of the Standard Model (SM) such as its flavour

[2]Long Shutdown 3, currently scheduled over 2026 - 2027 for the CERN injectors

structure, the mass pattern, the left-right asymmetry in the fermionic sector, and shed light on why the Planck scale, related to the universal gravitational interaction, is so large in comparison to the Fermi scale of the electro-weak interactions.

The state-of-the-art in theoretical and experimental particle physics, cosmology and astrophysics still leave the parameters of New Physics largely undetermined. We do not have a definitive prediction as to the masses, spins, and coupling constants of the associated new particles. For example, with regard to dark matter, the absence of detection in direct and indirect search experiments for weakly interacting massive particles (WIMPs) in the GeV-TeV mass range have stimulated growing interest in new experimental approaches that allow searching for light dark matter candidates, such as sub-GeV-mass WIMP-like particles, axions with masses from 10^{-20} eV to a few GeV and even more, sterile neutrinos with masses from a few keV and above, etc. The dark matter particle might also be part of a richer dark sector that connects to the SM through "portals" — particles that interact with both hidden and the SM sectors ([107] and references therein).

The fact that no convincing signs of new particles have been found so far suggests that they are either heavier than the reach of present-day accelerators or that they interact very weakly. This motivates searches for new physics by pushing *both* the high-energy frontier for potential detection of heavier and heavier particles, *and* the intensity frontier with searches for FIPs.

The search for FIPs, or long-lived new particles, is steadily gaining attention. Past experiments mainly searched for FIPs as a by-product of experiments developed for other purposes, often as a result of post-processing and data mining, and mostly with the capability limited to exclusion and not discovery. Searches for a wide range of FIPs, including heavy neutral leptons (HNL), dark photons (DP), dark scalars (DS), axion-like particles (ALP), light dark matter (LDM) and other super-weakly interacting light particles have now been included in the scientific goals of many presently running experiments. It has become an important part of the science programme at the LHC, as well as one of the objectives for the HL-LHC. Future colliders could drastically advance the intensity frontier, as increasing collision energies implies also increasing the number of W, Z and Higgs bosons and mesons — the particles that can efficiently produce FIPs in their decays.

However, to be detected, identified, and measured, new particles should decay or interact inside the detector with a significant probability. A common property of FIPs is that the distance they travel before decay grows fast when their mass gets smaller. As a result, this part of the parameter space for FIPs is practically inaccessible to collider experiments. Instead, the searches for New Physics in this region require experiments of a complementary type, having at least an order of magnitude longer fiducial volumes compared to collider detectors.The most developed type of such experiments are beam-dump experiments. Previous experiments of this type can only be considered as proofs of concept as their sub-optimal geometrical configuration resulted in very small acceptances. The beam-dump configuration also allows benefiting from the very high luminosity that can be achieved with an optimised long and high-density target system.

We argue here that the existing infrastructure at CERN can be upgraded to deliver 4×10^{19} protons at 400 GeV on a dedicated beam dump, achieving annual integrated luminosities that are more than three orders of magnitude higher than at HL-LHC. This gives access to for instance an order of magnitude higher annual yield of charm production in

the proposed detector acceptance than at HL-LHC. Together with modern technologies for background suppression and a general-purpose detector, we demonstrate that we can, with a detector designed for discovery, improve previous search results by $3-4$ orders of magnitude. This would significantly advance the intensity frontier in a complementary manner to the existing and future collider experiments. It's the purpose of BDF/SHiP to make a break-through in this direction during the next 10-15 years, in parallel with the HL-LHC programme.

During this period, a major inflow of astrophysical and cosmological data is expected. The data from cosmic and ground-based telescopes such as GAIA [137], DESI [138], EUCLID [139], Vera Rubin Observatory [140], E-ELT [141], JWST [142] and later SKA [143] might bring significant progress in the understanding of the properties of dark matter particles, such as mass and quantum wave length, free streaming, cross-section of self-interaction, and life time (for more details see [145-150]). Combining this with the discoveries or limits on interactions between hidden sectors and the SM sector that can be obtained at BDF/SHiP becomes a powerful tool for guiding the future strategies and technology developments in both fields (see e.g. [151,152]).

The BDF/SHiP physics programme was explored in a dedicated physics book in 2015 [11,107] by a large collaboration of theorists and has been further elaborated over the years, culminating with the comprehensive coverage of the field in the ESPPU2020 Physics Briefing Book [129]. Beyond the exploration of FIPs, BDF/SHiP is also particularly suitable for a rich program of tau-neutrino physics and measurements of neutrino-induced charm production [2,4,11]. It has also been shown that the BDF/SHiP target system can give unique access to a high-intensity neutron spectrum [3] that is not easily accessible at spallation facilities. This makes it possible to implement a user platform [153] for studying neutron-induced reactions on short-lived isotopes that is relevant for astrophysics [154], material testing [155], and radiation-to-electronics (R2E) studies.

3 Overview of BDF/SHiP at ECN3

3.1 Beam dump facility

The design and technology studies, including prototyping, for BDF have been documented in detail in the Comprehensive Design Study report and other documents in Refs. [**3**,**29**,15-28,30-40]. The implementation in the existing TCC8 and ECN3 reuses the designs developed for the original proposal. Only the most relevant aspects for the implementation in ECN3 are reported below.

At the SPS, the optimal experimental conditions for BDF/SHiP are obtained with a proton beam energy of 400 GeV and slow extraction of the proton spills over one second. The design of the BDF is based on returning to the full exploitation of the CERN accelerator complex with the SPS at its present performance. The SPS serves the LHC (HL-LHC) and a set of fixed-target facilities for physics and for R&D, together using up to 1.5×10^{19} protons per year. Since the completion of the CNGS project in 2013, up to 4×10^{19} protons per year at 400 GeV have been left available but unexploited. At a nominal spill intensity of 4×10^{13} protons, and 10^6 spills per year, up to 2×10^{20} protons on target could be delivered to BDF in about five years of nominal operation, while respecting the requirements of the

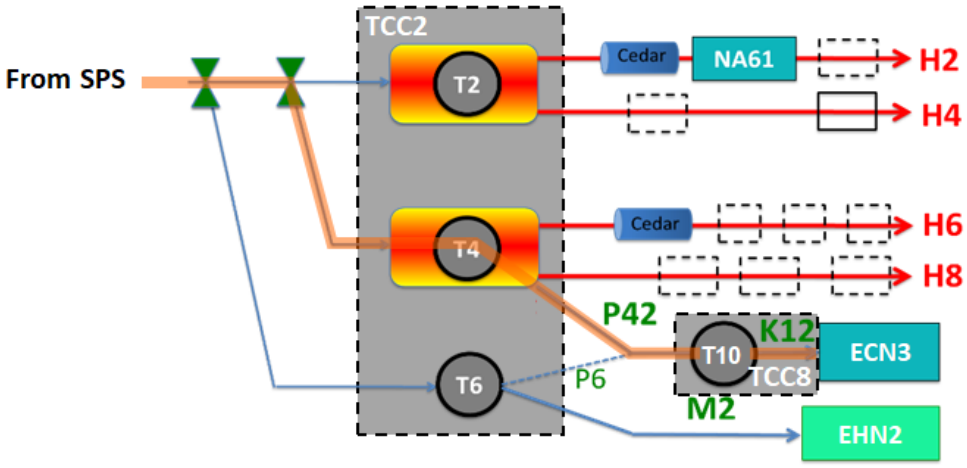

Figure 1: Overview of the North Area beam lines, targets and beam facilities.

HL-LHC operation as well as all the other existing beam facilities [32]. The recent upgrades of the SPS may lead to the capability of delivering more than 4×10^{13} protons per spill in the future, potentially allowing BDF to receive up to 3×10^{20} protons on target in five years of operation [156,157].

Fig. 1 shows an overview of the North Area beam lines. The TCC8 target hall and the ECN3 experimental area are located at the end of the P42 beam line. The present T10 production target in TCC8 would be removed along with the entirety of the K12 kaon beam line. The T4 target, located in the TCC2 target hall, serves the H6 and H8 beam lines by intercepting a fraction of the current primary proton beam sent to TCC8/ECN3. The delivery of BDF/SHiP's requirements could be realised by transferring the primary proton spills past the T4 production target and into the P42 beam line on dedicated SPS North Area cycles. The technical feasibility of the target bypass is being investigated by the PBC ECN3 Beam Delivery Task Force [131] via either (i) a closed vertical orbit bump or (ii) by actuating the target within the SPS supercycle. A decision on the concept to be employed is expected early 2023 with the installation of a prototype bumper system for tests with beam. At the upstream end of TCC8, the magnets of the BDF dilution system would be installed along with a vacuum chamber spanning the length of TCC8 towards the BDF/SHiP proton target, with the ∼130 m drift distance exploited to increase the beam size and develop the dilution pattern on the target's front face.

The layout of BDF/SHiP at the end of TCC8 and throughout ECN3 is shown in Fig. 2. The setup consists of the high-density proton target, effectively acting as a beam dump and absorber, followed by a hadron absorber and a magnetic muon shield immediately downstream [71,72]. The shield deflects the muons produced in the beam dump in order to reduce the flux in the detector acceptance to an acceptable level. The hadron absorber is an integral part of the overall shielding that is completely surrounding the target system. Together they form a compact and free-standing target complex, shown in Fig. 3.

The target complex design draws from the experience gained during the CDS phase [21,34]. Significant simplification and reduction in shielding is possible thanks to the use of an already operational underground area and thanks to the depth of TCC8. The helium vessel containing the proton target and the proximity shielding may be substituted either by a nitrogen

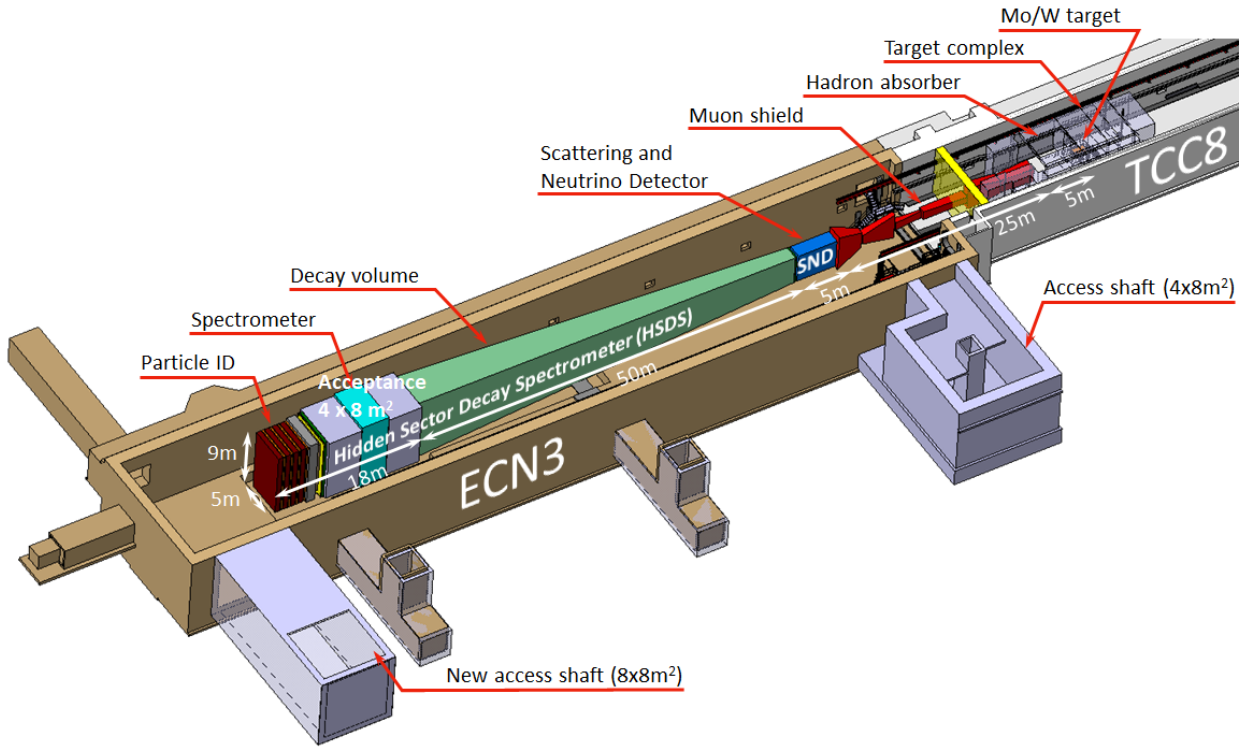

Figure 2: Overview of the BDF/SHiP experimental setup in the SPS TCC8/ECN3 beam facility.

system or a vacuum vessel. The handling of the target systems may be carried out by the existing crane in TCC8, taking inspiration from the recently developed design of the new SPS beam dump [160,161]. This has led to a revision of the shielding and the system handling in ECN3 to cope with the space and access constraints, while fully respecting the constraints from radiation protection.

The dynamic air confinement around the target complex would be guaranteed by two walls acting as ventilation partitions. The walls would also respect the fire safety requirements as outlined in the FIRIA Project [158]. The target complex could potentially house additional infrastructure, such as a lateral radiation port, that would allow using the significant neutron fluence emerging from the production target for physics or for mixed-field neutron irradiations [153] for accelerator and material science applications.

In order to maximise the production of heavy flavoured hadrons and photons, and at the same time provide the cleanest possible background environment by suppressing decays of pions and kaons decaying to muons and neutrinos, the target should be long and made from a combination of materials with the highest possible atomic mass and atomic number, and be optimised for maximum density with a minimum of space taken by internal cooling. The corresponding target system developed during the CDS phase [16,19,22,38] requires no modifications with respect to the implementation in ECN3. The baseline design is still composed of blocks of titanium-zirconium-doped molybdenum alloy (TZM), cladded by a tantalum-alloy, in the core of the proton shower, followed by blocks of tantalum-cladded pure tungsten. The blocks are interleaved with a minimum number of 5 mm gaps for cooling,

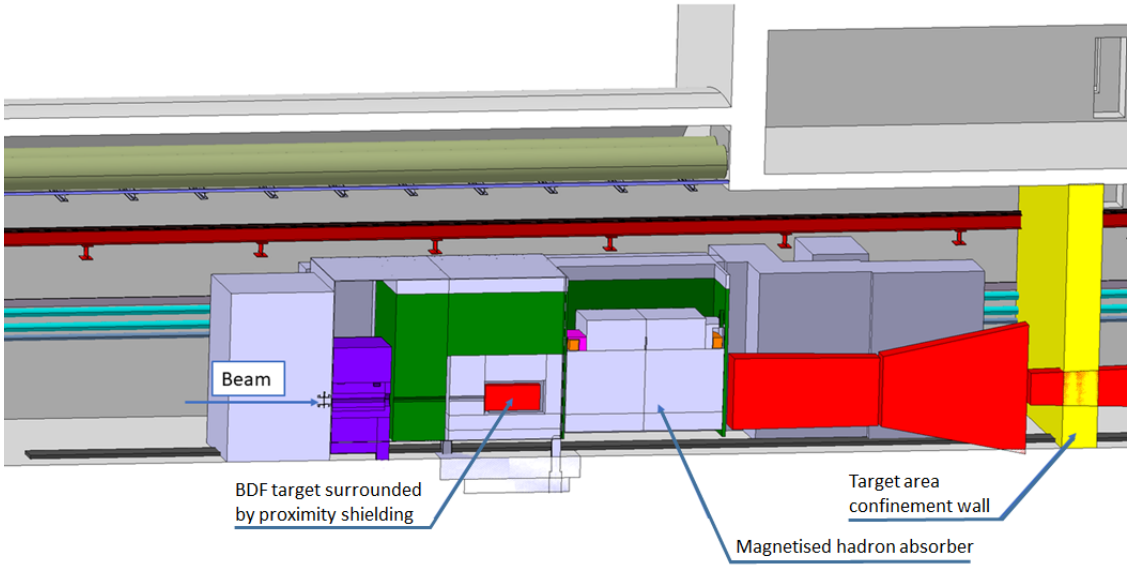

Figure 3: Preliminary design of the BDF-SHiP target area implemented in ECN3.

resulting in a total length of twelve interaction lengths.

The five metres long hadron absorber, made of iron, absorbs hadrons and electromagnetic radiation emerging from the proton target. The hadron absorber is equipped with a coil which magnetises the iron shielding blocks to serve as the first section of the active muon shield [71,72]. The rest of the muon shield consists of free-standing magnets. The target complex and part of the free-standing muon shield is located at the end of the TCC8 target hall, while the subsequent muon shield magnets are located in the taller ECN3 experimental hall.

The implementation of BDF/SHiP in ECN3 has undergone a first series of radiation protection studies by detailed FLUKA Monte Carlo simulations [162,163]. These studies have been aimed at optimising the implementation in TCC8 and ECN3 to ensure that the exposure of personnel and members of the public to radiation, as well as the radiological impact on the environment, would be as low as reasonably achievable (ALARA [159]). Thanks to the in-depth studies of the CDS, a new design profiting from the existing underground areas TCC8 and ECN3 could be quickly proposed. Relative to the original CDS design, it has been possible to reduce the amount of shielding at strategic locations by benefiting from the thick soil layer above TCC8 and ECN3 and the already existing shielding. Consequently, decommissioning would also involve less newly produced radioactive waste. Preliminary studies of prompt radiation above the target complex demonstrate that dose rates are well below the limit for non-designated areas. Furthermore, the doses due to stray radiation at the CERN fence downstream of ECN3 and beyond were investigated. Preliminary results show that the ambient dose equivalent limit for the CERN fence would not be exceeded and that the effective dose to the representative person from the public would remain well below the de Minimis value of 10 µSv/y. Activation and contamination of groundwater and soil has been taken into account in the shielding design as well. However, due to lack of information about the groundwater transport, very conservative constraints on the activity concentration have been applied. A hydro-geological study could provide the information

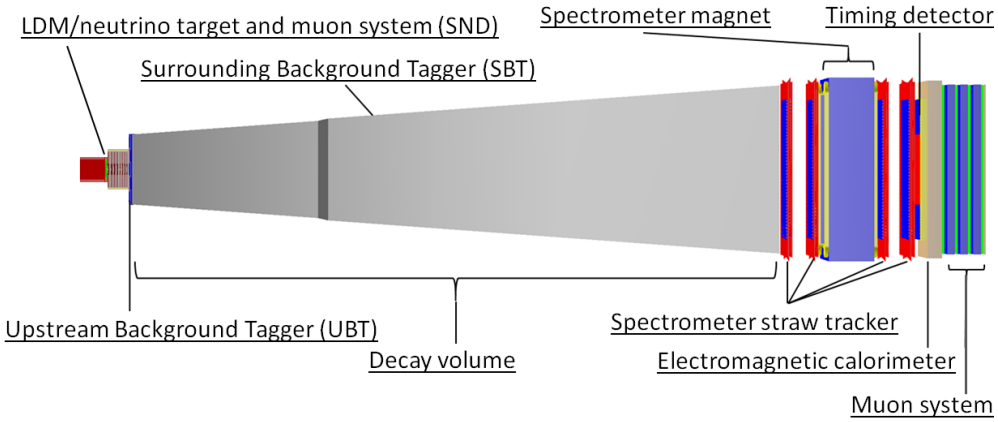

Figure 4: Schematic layout of the Scattering and Neutrino Detector (SND) and Hidden Sector Decay Spectrometer (HSDS).

needed to remove the excessive conservatism and to further reduce the required shielding. Residual dose rates in the target area were evaluated for five years of nominal operation and 2×10^{20} protons on target, showing that the target area is sufficiently shielded. Studies are underway of air and nitrogen/helium activation occurring inside of the nitrogen/helium target vessel and the surrounding air. The design of the associated ventilation system shall guarantee that air release has negligible radiological impact on the public.

From the studies performed during the CDS phase, the radiation to the detector electronics in ECN3 is expected to be significantly below levels that require special measures.

3.2 SHiP detector

A detailed description of the detector, the design and the detector performance from measurements with prototypes in test beam have been reported in Refs. [**2,4,46**,41-45,47-76]. Below is a summary of the most relevant features of the SHiP detector.

The SHiP experiment is composed of a dual system of complementary apparatuses, shown in Fig. 4. The upstream system, the Scattering and Neutrino Detector (SND), is designed to search for LDM scattering and perform neutrino physics. The downstream system, the Hidden Sector Decay Search (HSDS) detector is designed to reconstruct the decay vertices of FIPs, measuring invariant mass and providing particle identification of the decay products in a nearly zero background-level environment.

The SND detector consists of a LDM/neutrino target with vertexing capability incorporated in the form of tungsten plates alternated with emusion films and fast electronic detector planes. In the CDS design, the target region was magnetised, thus enabling momentum and charge measurements of muons and charged pions and kaons. The target region is followed downstream by a muon identification system. The electronic detector planes in the target region are based on scintillating fibres and have a spatial resolution of 50 µm and single-plane time resolution of 400 ps. The configuration allows reconstructing the shower produced by the recoil electron in LDM scattering to determine the initial particle angle and energy. In addition, the micro-metric accuracy of the nuclear emulsion provides crucial topological discrimination of LDM interactions against neutrino-induced background events.

For the neutrino physics programme, the emulsion technique allows detecting tau leptons and charmed hadrons by disentangling their production and decay vertices with the help of the sub-micrometric position and milliradian angular resolution. The SND muon system is designed to identify muons produced in the ν_τ interactions in the golden mode $\tau \to \mu\nu_\tau\overline{\nu}_\mu$ at high efficiency. A magnet around the LDM/neutrino target was foreseen in the CDS design to distinguish between interactions of ν_τ and anti-ν_τ by reconstructing the charge in the τ decays to hadronic final states, and to also measure the momenta of pions and kaons for the total hadronic energy measurement.

The HSDS detector measures both fully reconstructable decays of FIPs as well as partially reconstructable decays with neutrinos in the final state in a 50 m long decay volume of a pyramidal frustum shape.

The HSDS decay volume is followed by a large spectrometer. The main element of the spectrometer is the straw tracker, designed to accurately reconstruct the decay vertex, the mass, and the impact parameter of the reconstructed FIP trajectory at the proton target. The spectrometer dipole magnet provides a total field integral of about 0.5 Tm. The initial design of the magnet was based on a normal-conducting coil [58]. In order to significantly reduce the power consumption, the CDS phase included a study of a new type of high-temperature superconductor-based design [52] that is aimed at providing the same field gradient. An R&D programme with the goal of developing a demonstrator is currently starting up at CERN with the involvement of a SHiP institute [164].

An electromagnetic calorimeter (ECAL) and a muon detector provide particle identification, which is essential in discriminating between the very wide range of models with FIPs, but also in providing information for background rejection. The ECAL is a scintillator/lead sampling calorimeter, consisting of two parts of $3\,X_0$ and $17\,X_0$, respectively, which are mechanically separated by 1 m in the longitudinal direction. Each part is equipped with a high spatial resolution layer in order to precisely measure the shower axes and allow reconstructing the vertex of ALP$\to \gamma\gamma$ decays and the invariant mass. Measurements of shower profiles with a prototype in test beam show that an angular resolution of $15/\sqrt{E[\mathrm{GeV}]}$ mrad is achievable. The longitudinal segmentation of the ECAL also improves the electron/hadron separation. The muon system consists of four stations interleaved by three muon filters.

The key feature of the HSDS detector design is to ensure efficient control and suppression of the different backgrounds. Background from neutrinos interacting within the decay volume is eliminated by maintaining the decay volume at a pressure of ~ 1 mbar. The decay volume wall is instrumented upstream and on the sides by a system of high-efficiency background taggers in order to provide regional veto against muon and neutrino interactions in the vessel walls and against particles entering the volume from outside, including cosmics. The taggers covering the surrounding walls (SBT) are based on a liquid scintillator system segmented in cells with a thickness of 30 cm. Recent test beams have shown that the thickness can be reduced without affecting the performance. A threshold of 45 MeV is applied for the energy deposition, resulting in an efficiency of >99% and a $\sim$ns time resolution for the SBT. The tagger on the upstream vessel wall (UBT) is based on two 6-layer MRPCs, each with 100 ps resolution, 98% efficiency and spatial resolution of a few millimetres. A dedicated timing detector is located between the last spectrometer tracker plane and the ECAL to provide a measure of time coincidence in order to reject combinatorial backgrounds. It is based on scintillating bars and has a time resolution of $\sim$100 ps. Due to the criticality of the

veto systems and the timing detector, they have been through several test-beam campaigns, including measurements with large-scale prototypes.

3.3 Detector revision and implementation in ECN3

The suppression of physics background in SHiP is based on a combination of minimising the beam-induced particle rates in the detector acceptance by the highly optimised target design, hadron absorber and muon shield, and rejecting residual backgrounds by applying veto taggers, temporal, spatial and kinematics cuts, and particle identification in the detector.

For the optimisation in the CDS phase, a working point was chosen that put emphasis on the muon shield, while relying on only loose selection criteria based on the detectors, hence leaving a high level of redundancy in the overall background suppression. The revision of SHiP for the smaller ECN3 experimental hall has started from a simple shortening of the muon shield in the first iteration, shifting the working point for the combined background suppression towards a slightly higher reliance on the detector, in particular on the veto systems. As a result of bringing the experiment closer to the proton beam dump, the detector can be reduced in lateral size while the signal acceptance is preserved for all physics modes, production and scattering/decay kinematics convolved together. Thus far, in order to remain conservative, the adaptation for ECN3 has made no assumptions about using magnet technologies for the muon shield that allow higher field gradients than conventional warm magnets.

With respect to the CDS design, the muon shield has been shortened by more than 5 m to a total length of about 25 m. The space for the SND detector has also been reduced. In the current configuration, the magnet around the LDM/neutrino target has been removed. Instead a magnetised muon system is considered in order to distinguish between ν_τ and $\overline{\nu}_\tau$. Without the magnet, the momentum of charged pions and kaons would be measured through the detection of their multiple Coulomb scattering in the target [165]. In addition, the muon system would be designed to also serve as a hadronic calorimeter to obtain an inclusive energy measurement. The LDM/neutrino target mass and shape is under study to preserve the yield for the LDM search and the neutrino physics.

The shorter distance between the beam dump and the decay spectrometer allows reducing the aperture of the HSDS spectrometer from the original 5 m width and 10 m height to $4 \times 8\,\mathrm{m}^2$, consequently reducing also the decay volume and the particle identification systems in height and width. The lengths of the decay volume and the detector systems remain unchanged.

The updated dimensions of the muon shield and the detectors allow integrating SHiP in the existing TCC8/ECN3 hall below the existing bridge cranes in TCC8 and ECN3. While the distance between the Salève-side wall and the decay volume in ECN3 is between $\sim 4-2$ m (upstream/downstream), the Jura-side wall is at about the same distance of $\sim 9-7$ m as in the original CDS design.

Limited modifications to the ECN3 floor will be necessary under a part of the decay volume and under the spectrometer/particle identification systems. A detailed investigation of the impact and reuse of existing services and infrastructure has been performed. The implementation of BDF/SHiP will not interfere with services for other facilities on the North Area and a number of existing detector services may be reused. The current surface buildings

appear sufficient to host detector electronics and computing, and space for operating the detector.

4 Physics performance

The BDF/SHiP physics performance is anchored in a highly efficient background suppression, provided by the design of the target, hadron absorber and the muon shield. The background suppression is further guaranteed by the detector systems and, in the case of the search for FIP decays, also by maintaining the decay volume under vacuum. The overall detector concept provides sensitivity to as many decay modes as possible to ensure model-independent searches.

In addition to improving present constraints on many models by several orders of magnitude, the SHiP decay spectrometer allows distinguishing between different models, and, in a large part of the parameter space, measure parameters that are relevant for model building and cosmology. These features make BDF/SHiP a unique direct-discovery tool for FIPs. Moreover, together with the direct search for LDM, and neutrino physics, BDF/SHiP represents a wide scope general-purpose beam-dump experiment.

All physics sensitivities below are based on acquiring 2×10^{20} protons on target, which is achievable in five years of nominal operation at ECN3 with the currently unexploited proton yield from the SPS [32].

4.1 Simulation and reconstruction

The expected physics performance in ECN3 has been studied in detail with the help of the full GEANT-based Monte-Carlo framework that was developed for the original proposal. The detector responses have been tuned with the measurements done in test beams with prototypes of all subdetectors during the CDS phase. Extensive simulations of the background components were done in order to study the backgrounds generated by muon and neutrino deep inelastic scattering (DIS) in and around the detector, and by combinatorial events from residual muons. For the implementation in ECN3, the simulation has been updated with the complete geometry of the underground complex and the revised muon shield and detectors. The ECN3 background evaluation and signal yields have been obtained in a rerun of the background samples through the new geometry and analysis chain.

The SHiP software framework for simulation, reconstruction, and analysis is based on the FairRoot package [166] and is called FairShip. The framework incorporates GEANT4 [167,168] to simulate the particles through the target and the experimental setup, PYTHIA8 [171] for the primary proton fixed-target interaction, PYTHIA6 [169,170] for muon deep inelastic scattering and cascade production of charm and beauty [87], and GENIE [172] for interactions of neutrinos. The production and decays of various types of FIPs have been implemented in FairShip. Mainly PYTHIA8 is used to generate the different signal processes.

A total of 6.5×10^{10} protons on target have been simulated with an energy cut of 10 GeV for transporting particles after the hadron absorber. This simulation was run with strongly enhanced muon production from QED processes, such as resonance decays and

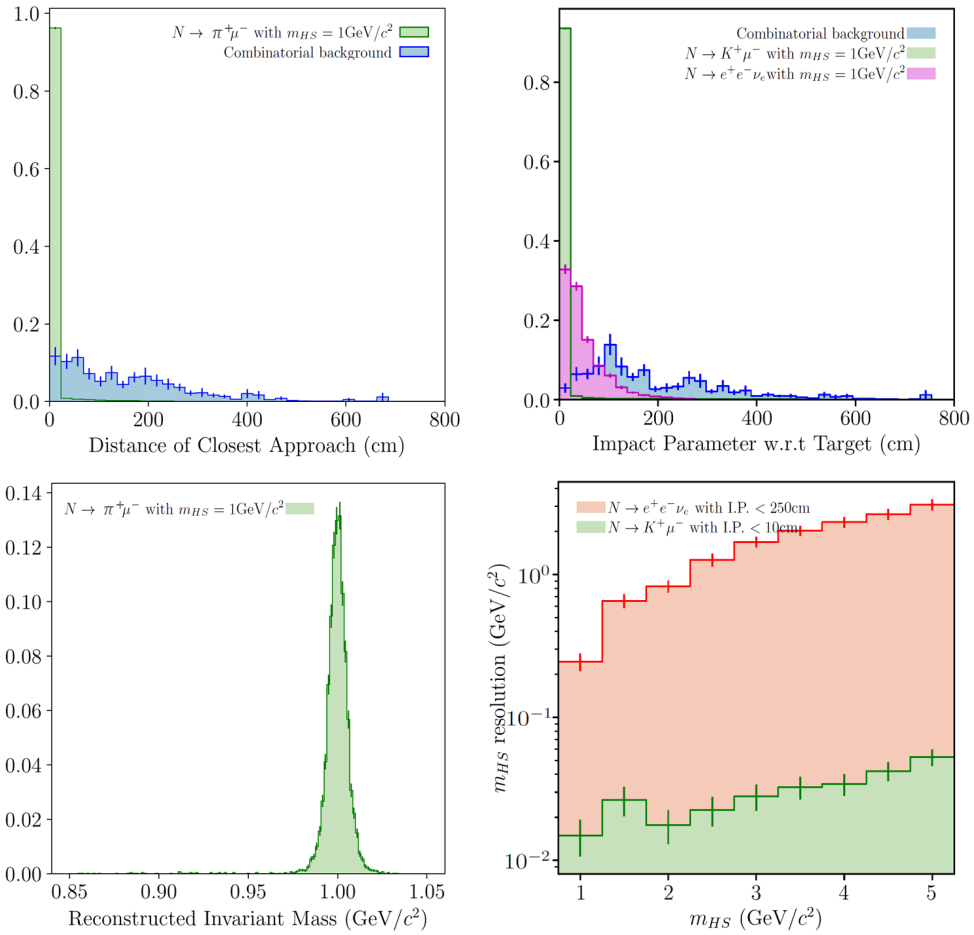

Figure 5: Examples of detector performance showing key reconstructed observables for an HNL candidate of $m_{HS} = 1\,\text{GeV/c}^2$ decaying to fully reconstructed modes and to partially reconstructed modes with neutrinos. For the distance of closest approach (top-left) and impact parameter (IP) with respect to the proton interaction region (top-right), both the signal (green and pink) and combinatorial background (blue) distributions are shown. Details on the combinatorial background can be found in Section 4.3.1. All distributions are normalised to unit area. Bottom-left shows the reconstructed invariant mass and bottom-right the mass resolution as a function of the HNL mass.

gamma conversion. For the studies of muon-induced backgrounds, the sample corresponds to 6.5×10^{12} protons on target. In addition, a total of 1.8×10^9 protons on target have been simulated with an energy cut of 1 GeV. Dedicated samples of charm and beauty hadrons corresponding to about 10^{11} protons on target have been produced. These simulation samples give sufficient statistics after the muon shield for the background determination to be extrapolated to the full run of BDF/SHiP with 2×10^{20} protons on target with good statistical accuracy and such that any rare contribution to the muon flux is subdominant.

In order to produce a background sample of muon DIS events that is equivalent to what is expected for the full run of BDF/SHiP, the muon samples from the simulations above were used to produce DIS events with the cross-section boosted such that every muon interacts according to the material distribution of the experimental setup.

For neutrino DIS, the neutrino spectra from the simulated minimum bias, and charm and beauty samples were used to produce a sample of neutrino interactions in the material of the detector with the help of the GENIE generator that is equivalent to seven times the full run of BDF/SHiP, again by forcing every neutrino to interact according to the material distribution of the experimental setup.

The validity of the FairShip prediction of the particle fluxes has been verified by comparing to the data from the CHARM beam-dump experiment at CERN [173]. The most realistic cross-check of FairShip has been performed in summer 2018 in a dedicated experiment at the CERN SPS [9]. It has directly measured the rate and momentum of muons produced by 400 GeV/c protons dumped on a replica of the BDF/SHiP target, and found a very good agreement between the prediction by the simulation and the measured spectrum [80].

A key goal of the SHiP detector is to perform accurate reconstruction of the events. On the one hand, it allows precisely determining the mass of a potential hidden sector candidate. On the other hand, accurate vertex and momentum resolution are critical to suppress backgrounds. As FIP candidates originate from the target, the impact parameter of the reconstructed candidate with respect to the proton interaction region ($\mathrm{IP}_{\mathrm{target}}$) offers excellent discriminating power against backgrounds. In addition, signal tracks originate from a common vertex in contrast to backgrounds arising from random combinations of tracks. Therefore, the distance of closest approach (DOCA) between tracks can also be used to suppress backgrounds. GENFIT [174] is used for reconstruction of tracks in the FairShip reconstruction framework. The distributions of $\mathrm{IP}_{\mathrm{target}}$ and DOCA for typical signals and combinatorial background are shown in Fig. 5. The mass resolution of an HNL candidate with mass 1 GeV/c^2 reconstructed through the decay HNL$\to \mu^{\pm}\pi^{\mp}$ is also shown, together with the dependence of the mass resolution as a function of the mass of the HS particle for decays to both fully and partially reconstructed modes.

4.2 Muon shield performance

The goal of the muon shield is to reduce the initial flux of about 10^{11} muons per proton spill by up to six orders of magnitude. In the CDS design, the shield consisted of the magnetisation of the hadron absorber together with a chain of six normal-conducting magnets. The magnets were optimised in shape by using machine-learning techniques [72] and iterative simulation of the muon background sample to minimise the muon flux through the SND detector and the HSDS detector. The initial strategy for the shortening of the muon shield for ECN3

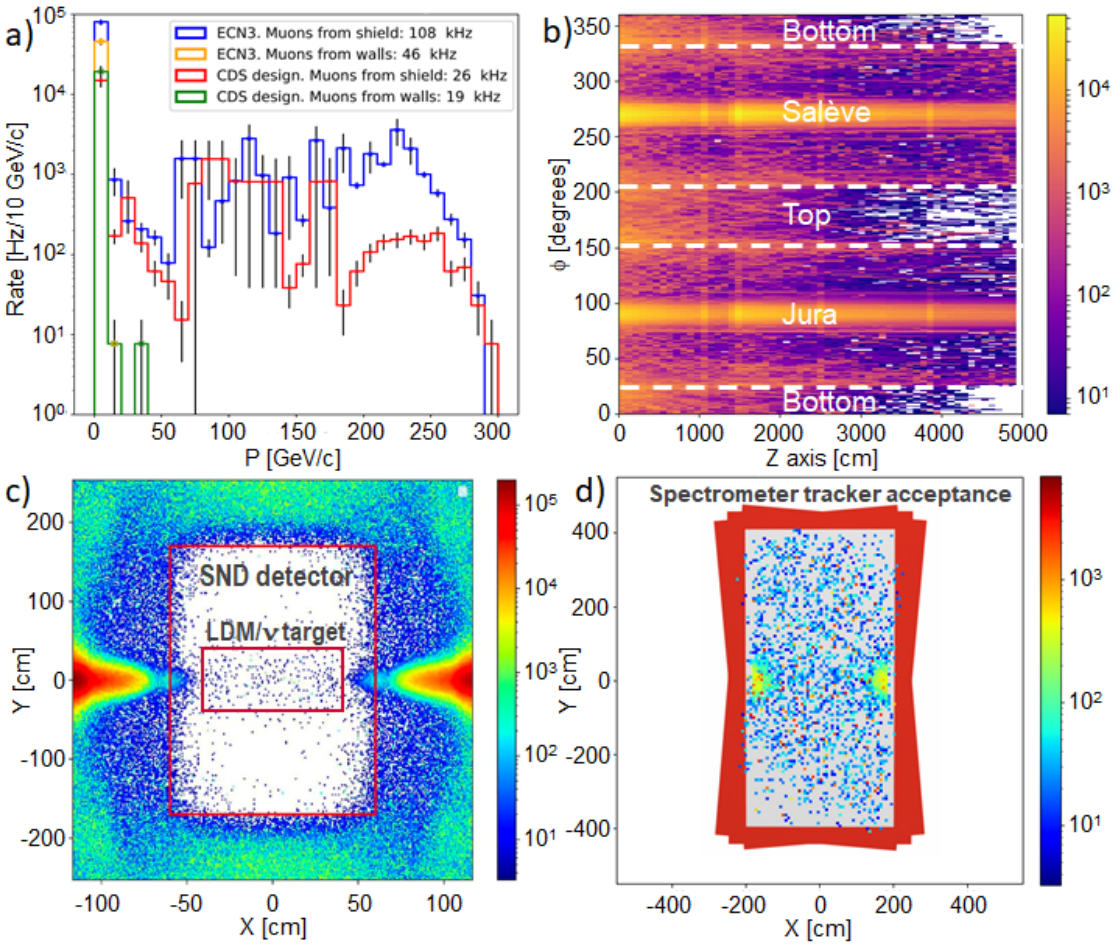

Figure 6: a) Rates against momentum of muons reconstructed in the HSDS spectrometer, comparing the rates in ECN3 with the shortened muon shield against the CDS design. The rates from muons scattering off the cavern walls are shown separately. b) SBT, c) SND and d) spectrometer tracker muon rate maps. For the SBT, ϕ counts clockwise from the bottom-centre of the decay volume.

has consisted in preserving the length and horizontal bending power of the hadron absorber and the first three free-standing magnets from the CDS design, and only updating the last three magnets by a simple down-scaling of their lengths. Fig. 6a shows a comparison of the muon spectrum per spill in the CDS design and in ECN3 as seen by the HSDS main tracker. "Muons from walls" are defined as those that are not directly coming from within the volume of the last muon shield magnet. As expected the rates have increased, overall by a factor between three and four with the simple length-scaled muon shield. As shown, the field integral of the shorter shield is still sufficient to deflect the hardest muons. The rate increase is primarily due to sub-optimal performance to re-deflect the mid- and high-momentum muons that have been swept out in the first half of the shield and then bent back towards the detector by the return field. To a lesser extent, the increased rate also comes from muons scattering in the Salève-side wall of ECN3. These muons arrive at the detector with momenta below 10 GeV/c. Fig. 6b shows the muon hit rate on the SBT by plotting

the cells clock-wise around the vessel and along its entire length. It also reflects the slightly higher rates from the closer Salève-side wall at $\phi = 270°$, with respect to the Jura-side wall at $\phi = 90°$. Fig. 6c and 6d show the resulting rate maps at the level of the SND detector and the HSDS main tracker. The region occupied by the SND detector in the ECN3 setup and the $80 \times 80\,\mathrm{cm}^2$ LDM/neutrino target of the CDS design are outlined in Fig. 6c. With the shortened muon shield, the rate within the target region is roughly 50 kHz. Past test beams and the experience with SND@LHC [180] show that the emulsion technology will work in these conditions.

Despite its weaknesses in providing an optimal deflection of muons of all momenta, the simple length-scaled version has been conservatively used for the full re-evaluation of the backgrounds in ECN3. The more time consuming work of performing a full optimisation of the muon shield has started in parallel. The first complete run with machine learning has already produced a version which further suppresses the rates by a factor of two but it has not been possibly to use it for this LoI due to the limited time.

Beyond the current investigations and technology, there are also reasons to believe that the use of superconducting (SC) magnets could result in important advantages. First explorations in this direction were done during the CDS phase and have continued in the context of ECN3 [41,42,44]. Both a one-magnet solution with unconfined return field, and an alternate polarity two-magnet solution with confined field have been considered. Preliminary results are encouraging. They indicate that, taking advantage of the stronger fields reachable with SC magnets, a substantial reduction in the length of the muon shield could be obtained. It opens up room to further improve the acceptance of the experiment.

These first explorations of a compact SC muon shield must be brought to the next level, taking into account engineering aspects, in order to obtain realistic designs and perform a full comparison with the baseline solution, including cost and performance.

4.3 FIP decay search performance

Efficient exploration of the wide range of possibilities and the parameter space for FIP decays is only possible if the backgrounds are well-controlled and reduced to negligible levels. The broad range of signals to which the SHiP experiment is sensitive can be classified into two main categories: fully and partially reconstructed decays. The former category refers to decays where there are at least two charged particles and no invisible final state particles, examples are DP$\rightarrow \mu^{\pm}\mu^{\mp}$ and HNL$\rightarrow \mu^{\pm}\pi^{\mp}$. The latter category refers to decays with at least two charged particles and at least one invisible particle in the final state, e.g. HNL$\rightarrow \mu^{\pm}\mu^{\mp}\nu$. This category is unique to search for HNL mixing with the third generation, since the HNL decay final states will contain a tau neutrino. In all cases, the experimental signature consists of an isolated vertex within the fiducial volume with a total momentum vector that extrapolates accurately back to the proton interaction region for fully reconstructed final states, and with a wider distribution of impact parameters for partially reconstructed final states (see Fig. 5).

Criterion	Requirement
Track momentum	$> 1.0\,\mathrm{GeV}/c$
Track pair distance of closest approach	$< 1\,\mathrm{cm}$
Track pair vertex position in decay volume	$> 5\,\mathrm{cm}$ from inner wall
Impact parameter w.r.t. target (fully reconstructed)	$< 10\,\mathrm{cm}$
Impact parameter w.r.t. target (partially reconstructed)	$< 250\,\mathrm{cm}$

Table 1: Pre-selection criteria used for the background rejection and the sensitivity estimates in the analysis of FIP decays. These are the same as used in the CDS study.

4.3.1 FIP decay search background evaluation

The FIP decay search strategy is to have a very loose common pre-selection, shown in Table 1. It preserves close to 100% of the signal efficiency in fully reconstructed modes, while in general, the efficiency for partially reconstructed modes is around 70%. This was obtained by simulating the signals with the full simulation.

There are three main sources of background that can mimic the signature of FIPs: random combinations of residual muons within the same proton spill, muon DIS and neutrino DIS. With the use of the SBT, the background from cosmics has been proven to be negligible [12].

• **Muon combinatorial:** This type of background arises when two opposite-sign muons within the same proton spill appear to form a vertex and point back to the target. The higher rate of residual muons with the non-optimized muon shield in ECN3 implies that the SBT and UBT veto systems are more active in the background rejection. The total expected rate of muons in the spectrometer with momentum $p > 1\,\mathrm{GeV/c}$, and that either directly enter the fiducial volume of the HSDS, or enter via back-scattering in the ECN3 cavern, and that satisfy basic track quality (sum of hits in all tracking stations $ndof > 25$, and track fit $\chi^2/ndof < 5$), is 60 kHz. This leads to 9×10^{15} possible track pairs within the 1 s spill windows in 2×10^{20} protons on target (opposite-charge pairing not taken into account). The rejection power of applying the pre-selection cuts is 9.04×10^{-4}. Under the assumption of a flat time structure for the 1 s proton spills[3], the time coincidence of the pairs of muons in a time window of 340 ps, corresponding to more than 2.5 times the time resolution of the HSDS timing detector, provides a rejection of 3.4×10^{-10}. Applying the regional veto from the SBT and the UBT suppresses the background by a factor 7.7×10^{-7}. As a result, the muon combinatorial background is expected at the level of 2.1×10^{-3} events for 2×10^{20} protons on target.

• **Muon DIS:** Muons may interact inelastically in the material of the detector or in the surrounding infrastructure. These DIS interactions produce V^0s but also, more importantly, false V^0s due to random combinations of tracks from the same DIS interaction. Typically, $\mathcal{O}(10)$ particles are produced in these interactions. Given the small energy transfer, the DIS interactions lead to energetic products that are aligned with the direction of the incoming

[3]In reality, non-uniformity in the spill structure and the probability of this background can be measured by relaxing the timing criterion. A fast high-resolution spill structure monitor is also under study. The information from the monitor will be recorded with the data to have a continuous measure of this background probability. At the same time, significant progress has also been made in the context of the BDF studies to improve the SPS spill structure, and studies of new techniques are underway [15,17,24,30]

Background source	Expected events
Neutrino DIS	< 0.1 (fully) / < 0.3 (partially)
Muon DIS (factorisation)	$< 10^{-4}$ (fully) / $< 10^{-2}$ (partially)
Muon combinatorial	2.1×10^{-3}

Table 2: Expected background in ECN3 in the search for FIP decays at 90% CL for 2×10^{20} protons on target after applying the pre-selection, the timing, and the UBT and SBT veto. The neutrino- and muon-induced backgrounds are given separately for the set of criteria corresponding to the fully and partially reconstructed signal modes.

muon. Hence, muon DIS background is dominated by those originating in the material in the close vicinity of the fiducial volume. DIS background events from the walls of the cavern are very rare. Similarly to the muon combinatorial background, the non-optimized muon shield in ECN3 implies a higher rate of muon DIS events, and consequently more reliance on the veto systems. About 9×10^{10} muon DIS interactions are expected in the proximity of the fiducial volume for 2×10^{20} protons on target. After the pre-selection, roughly 1000 background events are expected for fully reconstructed signals and 2×10^5 for partially reconstructed signals, i.e. rejection factors of 1.1×10^{-9} and 2×10^{-6}. Out of these, only 2×10^{-3} events and 0.2 events, respectively, come from real V^0s (K^0_S, K^0_L, and Λ). The combined regional UBT and SBT veto allows reducing the muon DIS background to a negligible level, resulting in upper limits of 10^{-4} events for fully reconstructed signal and 10^{-2} for partially reconstructed signal events for 2×10^{20} protons on target.

• **Neutrino DIS:** Similarly to the muon DIS background, the dominant source of neutrino-induced background comes from neutrino DIS in the material close to fiducial volume. In order to avoid irreducible background from neutrinos interacting with the air molecules inside the vessel, a level of vacuum below 10^{-2} bar is sufficient. The remaining main sources come from interactions with the inner wall of the decay volume ($\sim 50\%$), the liquid scintillator ($\sim 25\%$), and the SND ($\sim 10\%$). As the acceptance is the same, but the detector is smaller and has less material, the background from neutrino DIS is expected to be smaller in ECN3 than in the CDS design [2]. For this LoI, the neutrino background was checked with a reduced sample compared to the full sample used in the CDS study, corresponding to seven times 2×10^{20} protons on target. As the results were fully compatible, the CDS expectation is quoted here. In total, about 3.5×10^7 interactions are expected in the CDS design from 2×10^{20} protons on target. By applying the pre-selection cuts together with the UBT and SBT, < 0.1 background events are expected for the fully reconstructed signals and 6.8 background events for the partially reconstructed signals. The latter background consists of photon conversions in the material. It can be easily eliminated by requiring an invariant mass of the pair to be larger than $100\,\mathrm{MeV/c^2}$.

In conjunction with the development of the selection criteria, it has been verified that the probability that an actual signal candidate is wrongly vetoed by an uncorrelated hit in the SBT remains insignificant. With the simple regional veto that requires the SBT hit to be upstream of the signal candidate vertex and within a time window of $3 \times \sigma_{\mathrm{SBT}}$ (time resolution $\sigma_{\mathrm{SBT}} \sim$ ns) the probability is roughly a percent.

In summary, we have studied the background in ECN3 with the full simulation and the whole detector and underground geometry implemented. The SHiP experimental setup

was designed with the concept of redundancy built in to the combined performance of the suppression of beam-induced particles rates and the detector.The adaptation to ECN3 and the results of the background studies bear witness of this strategy. The summary of the expected background levels is shown in Table 2, and does not differ significantly from the CDS results. The redundancy of the selection criteria would also allow determining the background directly from experimental data and, in case of signal evidence, to perform cross checks that minimise the probability of false positives.

4.3.2 FIP decay search sensitivities

The selection described above allows efficiently rejecting the backgrounds, and is entirely inclusive with respect to different types of long-lived particle decays in the fiducial volume. This ensures maximum sensitivity in the FIP searches, while remaining generic to new models that may be proposed in the future. Below, the sensitivities to six benchmark models [175] are calculated and used as proxies for generic FIP models. The corresponding sensitivity plots in Fig. 7 show the sensitivities in ECN3 compared to the CDS design. SHiP's sensitivity to axion-like particles with gluonic coupling is calculated for the first time.

HNL signal events were simulated for various masses and mixing elements $|U_{e,\mu,\tau}|^2$ with the SM electron, muon and tau neutrinos as the input parameters. The decays of HNLs to a large number of final states that contain at least two charged particles, were simulated using the HNL branching fractions from [81]. The sensitivity to various HNL benchmark models was estimated by applying the selection criteria in Table 1. Fig. 7a presents the sensitivity curve for HNLs, with the benchmark assumption that the ratio between the three HNL mixing angles corresponds to $(|U_e|^2 : |U_\mu|^2 : |U_\tau|^2 = 1 : 0 : 0)$. For HNL masses above $0.5\,\mathrm{GeV}/c^2$, the plot is also applicable for the muon-dominated mixing $(|U_e|^2 : |U_\mu|^2 : |U_\tau|^2 = 0 : 1 : 0)$. For completeness, both the conservative and the optimistic sensitivity contours are shown with the $b \to B_c$ fragmentation fraction set to $f_{b\to B_c} = 0$ and $f_{b\to B_c} = 2.6 \times 10^{-3}$, respectively. Below a mass of $0.5\,\mathrm{GeV}/c^2$, only production from D and B mesons is included. The curves take into account decays to $\ell^\pm\pi^\mp$, $\ell^\pm K^\mp$, $\ell^\pm\rho^\mp$, $\ell^\pm\ell'^\mp\nu$ for $m_N < 1\,\mathrm{GeV/c^2}$, and $q\bar{q}'\ell$, $q\bar{q}\nu$, $\ell^\pm\ell'^\mp\nu$ for $m_N > 1\,\mathrm{GeV/c^2}$. The fact that the signal yield scales with $|U_\ell|^4$, and since SHiP is a nearly zero background experiment, the 3σ sensitivity is close to the expected upper limit for 90% CL. In addition, in a large part of the sensitive region, SHiP could observe a large number of signal events. For instance, for a coupling of $|U|^2 = 2 \times 10^{-8}$, which is more than one order of magnitude below current limits, SHiP would observe 2600 events. Therefore, in case of discovery of HNLs, SHiP is capable of measuring parameters and identifying the underlying models. For instance, the left plot of Fig. 8 shows that SHiP may distinguish between Majorana-type and Dirac-type HNLs in a significant fraction of the parameter space by detecting lepton number violating or conserving decays [100]. If the mass splitting between the HNLs is small, the right plot shows that it may also be possible to resolve HNL oscillations as a direct measurement of the mass splitting between HNLs.

Dark scalars that mix with the SM Higgs can be produced in FCNC decays of b-hadrons. The sensitivity to dark scalars is shown in Fig. 7b. Inclusive decays of dark scalars are considered by using the inclusive $b \to SX_s$ branching fraction given in [99]. The final states included in the sensitivity are $\ell^+\ell^-$, $\pi^+\pi^-$, K^+K^-, 4π below $m_S < 2\,\mathrm{GeV/c^2}$, and $q\bar{q}$, gg above.

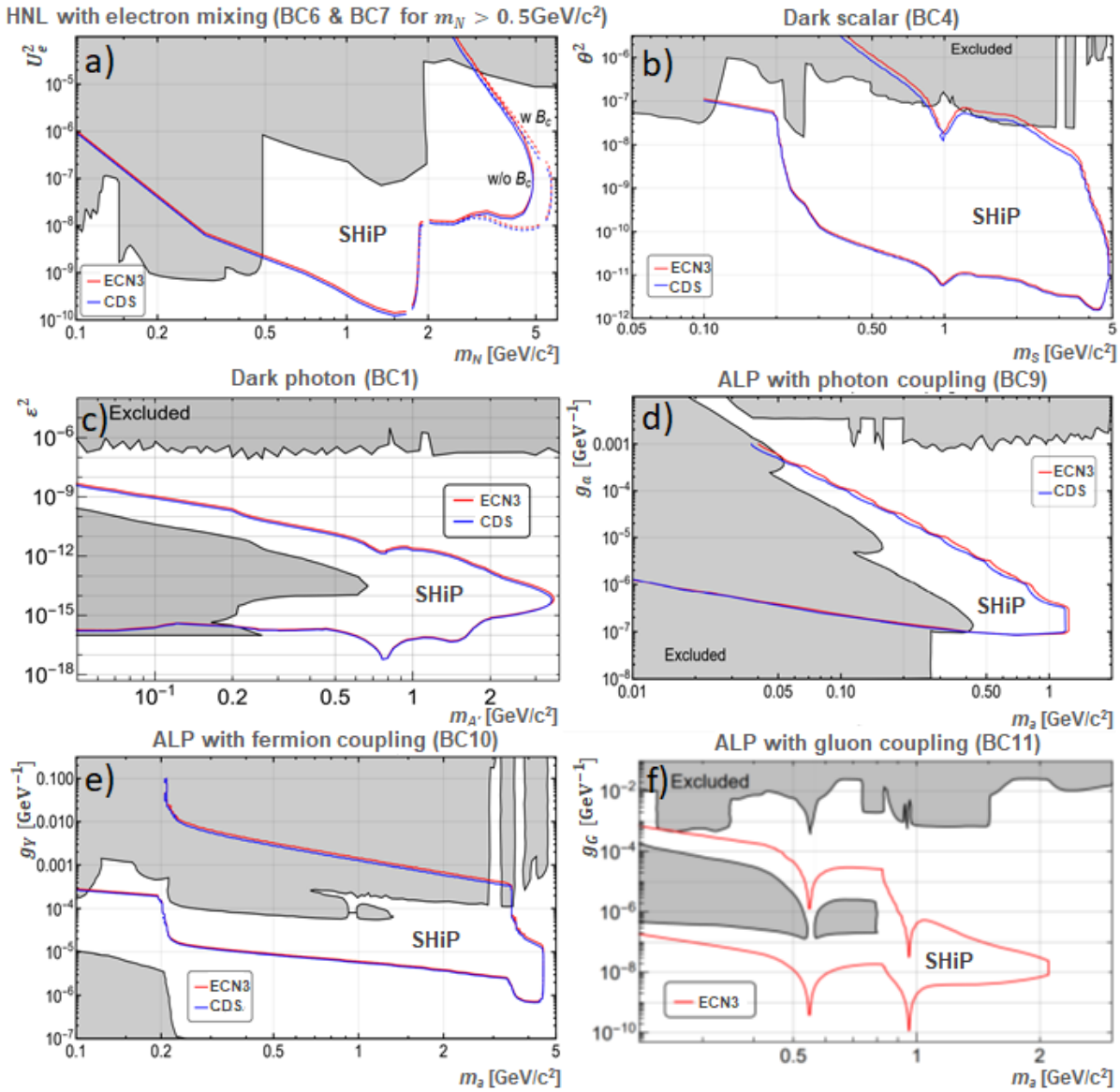

Figure 7: a) SHiP's sensitivity in ECN3 compared to CDS for HNLs, b) dark scalars for which only the contribution from B mesons is taken into account, c) dark photons from adding up the three production mechanisms described in the text, and axion-like particles coupled to d) photons, e) fermions, and f) gluons. All plots are based on 2×10^{20} protons on target and limits correspond to 90% CL. The benchmark models (BC) used are those in Ref. [175]. Regions shaded in grey are excluded by past and current experiments.

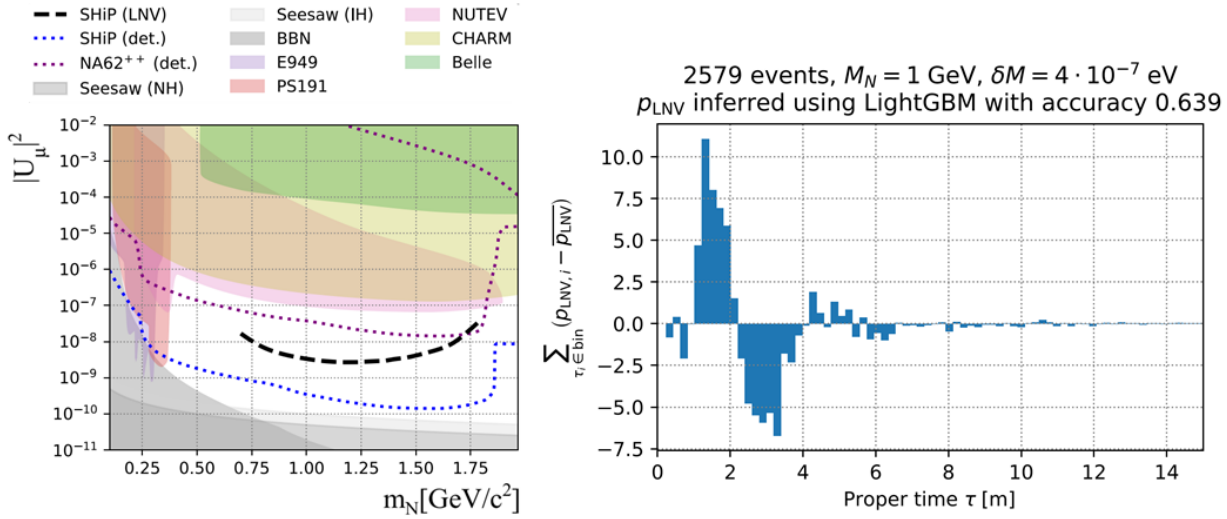

Figure 8: Left: lower bound on the SHiP sensitivity to HNL lepton number violation (black dashed line). Right: reconstructed oscillations between the lepton number conserving and violating event rates as a function of the proper time for a HNL with the parameters $M_N = 1\,\text{GeV}/c^2$, $|U_\mu|^2 = 2 \times 10^{-8}$ and mass splitting between HNLs of $4 \times 10^{-7}\,\text{eV}$. Both figures are from Ref. [100].

Three different mechanisms of dark photon production have been studied for estimating the sensitivity, considering at the moment only the primary proton interactions. The contribution from cascade production [87], which is included for the HNL and the dark scalar, and from electromagnetic showers is not currently taken into account for the dark photon, which makes the sensitivity estimate conservative. Dark photons with masses below $0.9\,\text{GeV}/c^2$ can mix with photons from neutral meson decays ($\pi^0 \to \gamma\gamma$, $\eta \to \gamma\gamma$, $\omega \to \pi^0\gamma$, $\eta' \to \gamma\gamma$) that are produced in non-diffractive interactions. PYTHIA8 is used to obtain an estimate of the neutral meson production rate. The proton interaction can also lead to the radiation of a dark photon via a bremsstrahlung process. This mechanism dominates for dark photon masses in the range $0.4-1.3\,\text{GeV}/c^2$. Above $1.3\,\text{GeV}/c^2$, the predominant production mechanism is quark-quark annihilation into dark photons. This process is simulated using a generic resonance that couples both to SM fermion pairs and feebly interacting particles, as implemented in PYTHIA8 for the "HiddenValley" Z' model [176]. The native cross section from PYTHIA8 is used for the normalisation of the process. The 90% CL exclusion contour shown in Fig. 7c adds up the three production modes studied. The sensitivity takes into account decays to leptons and hadrons. The description for hadronic decays was taken from Ref. [79].

For the sensitivity to ALPs, SHiP has used models with an exclusive coupling to photons, fermions, and gluons as benchmarks, Fig. 7d, e, and f, respectively. The final states taken into account are ALP(g_a) $\to \gamma\gamma$, ALP(g_Y) $\to \ell^+\ell^-$, and ALP(g_G) $\to \gamma\gamma$, $\eta/\eta'/\pi^0$-like decays for $m_{a_G} < 1.5\,\text{GeV}/\text{c}^2$, and above, only ALP($g_G$) $\to gg$. The photon channel requires the ambitious angular resolution of the ECAL to reconstruct the vertex and to cope with background from electromagnetic processes and background from neutrino interactions in the ECAL itself. The sensitivity is based on the angular resolution of $15/\sqrt{E[\text{GeV}]}\,\text{mrad}$.

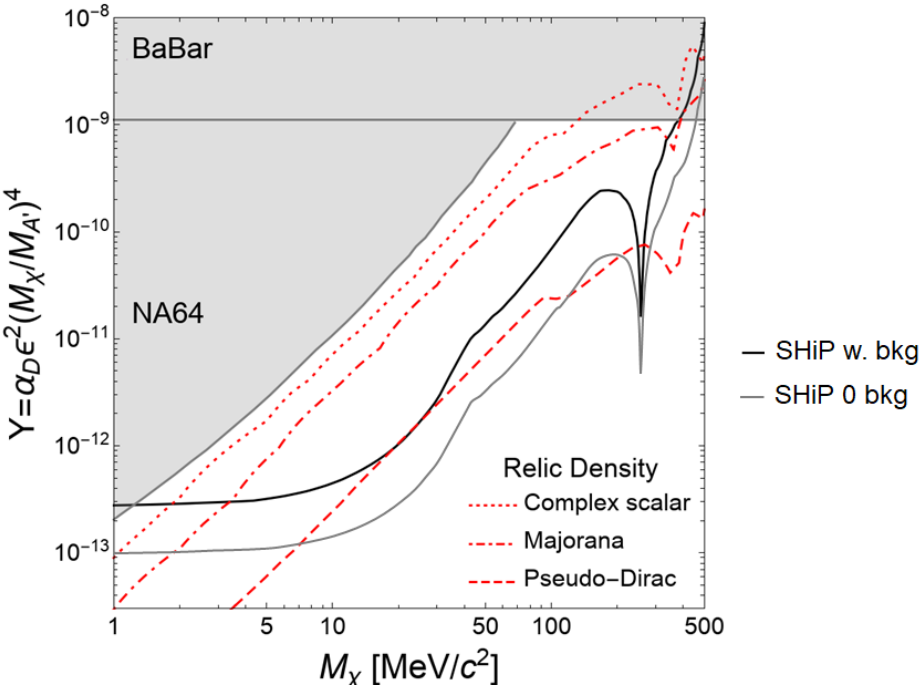

Figure 9: SHiP exclusion limits in the CDS design [78] at 90% CL as a function of the LDM mass M_χ, compared to the current experimental limits by NA64 [178] and BaBar [179] (grey shaded area) and the predicted thermal relic abundances for different dark matter particle types. The coupling is provided as $Y = \epsilon^2\alpha_D(M_\chi/M_{A'})^4$.

In summary, the re-evaluation of the background and the calculation of the signal yields above demonstrates that BDF/SHiP's sensitivity in ECN3 is practically identical to what was achieved in the original proposal. As before in the CDS, in most parts of the sensitive parameter space where at least a handful of events would be measured, BDF/SHiP is able to discriminate between the various models.

4.4 LDM search performance

The SND can probe existence of LDM (χ) by detecting the electromagnetic showers initiated by the recoil electrons coming from elastic scattering of LDM in the LDM/neutrino target. This was evaluated in the CDS design for an eight-tonne mass [2]. The mass and the shape of the LDM/neutrino target is currently being optimised, aiming at maximising the LDM sensitivity and the prospects for the neutrino programme. This LoI repeats the sensitivities already reported for the CDS design [78] for the eight-tonne target that was located at a larger distance from the proton dump than the corresponding location in the ECN3 setup.

Neutrino events with only one reconstructed outgoing electron at the primary vertex constitute background in the LDM searches, mimicking the signature $\chi e^- \to \chi e^-$. The GENIE Monte-Carlo generator [172], interfaced with FairShip, has been employed for a full simulation to provide an estimate of the expected background for 2×10^{20} protons on target. After imposing a selection optimised for the signal, the total residual neutrino background amounts to 230 events [78]. The dominant background contribution arises from

ν_e quasi-elastic scattering $\nu_e n \to e^- p$, where the soft proton remains unidentified, and from topologically irreducible sources, *i.e.* $\nu_e(\bar{\nu}_e)$ elastic and $\bar{\nu}_e$ quasi-elastic scattering ($\bar{\nu}_e\, p \to e^+ n$).

Signal events have been simulated with the help of the MadDump software [177], and assuming LDM pair-production ($\chi\bar{\chi}$) in the prompt decays of dark photons. In the considered dark photon mass range of $M_{A'} \sim \mathcal{O}(1\,\mathrm{GeV}/c^2)$, only contributions from the decay of light mesons (π, η, ω) and proton bremsstrahlung have been included. Prompt-QCD and heavier Drell Yan-like production mechanisms have been proven to be negligible. Assuming a benchmark scenario with relevant theory parameters corresponding to a dark coupling constant of $\alpha_D = 0.1$ and a LDM mass of $M_\chi = M_{A'}/3$, and a total of ~ 230 neutrino background events, the SHiP 90% CL sensitivity is computed in the plane (M_χ, $Y = \epsilon^2 \alpha_D (M_\chi/M_{A'})^4$), where ϵ is the dark photon coupling. Fig. 9 compares the SHiP sensitivity with the current experimental constraints and the thermal relic abundances, showing competitive limits in the considered region. The ultimate SHiP sensitivity for zero background is also shown.

In addition to the LDM sensitivity through electron recoil, detection of leptophobic dark matter/dark photons may also be possible through nuclear recoil. This has been studied in the context of the SND@LHC [180,181] and will be studied at SHiP in the future.

4.5 Neutrino physics performance

The nuclear emulsion technology combined with the information provided by the SND muon identification system makes it possible to identify the three different neutrino flavours in the SND detector. The neutrino flavour is determined through the flavour of the primary charged lepton produced in neutrino charged-current interactions. Compared to the CDS design [2], the suppression of the magnet surrounding the LDM/neutrino target for ECN3 implies that the discrimination between ν_τ and $\overline{\nu}_\tau$, based on the charge measurement in the subsequent τ-lepton decays, will not be possible in the hadronic decay modes. Instead, the charge measurement will be limited to the cleaner muonic decay mode with the help of the magnetised SND muon system. The loss in yield is compensated by the shorter distance to the target and by the possibility of re-dimensioning the LDM/neutrino target itself without the constraints from the magnet. This is currently under study.

The neutrino fluxes produced in the beam dump have been estimated with FairShip,

	CC DIS interactions	CC DIS w. charm prod.
N_{ν_e}	8.6×10^5	5.1×10^4
N_{ν_μ}	2.4×10^6	1.1×10^5
N_{ν_τ}	2.8×10^4	1.5×10^3
$N_{\overline{\nu}_e}$	1.9×10^5	9.8×10^3
$N_{\overline{\nu}_\mu}$	5.5×10^5	2.2×10^4
$N_{\overline{\nu}_\tau}$	1.9×10^4	1.1×10^3

Table 3: Expected CC DIS interactions in the SND in the CDS design with 2×10^{20} protons on target.

Decay channel	ν_τ	$\overline{\nu}_\tau$
$\tau \to e$	3500	
$\tau \to \mu$	1200	1000
$\tau \to h$	10 600	
$\tau \to 3h$	3700	

Table 4: Expected number of ν_τ and $\overline{\nu}_\tau$ signal events observed in the CDS design with 2×10^{20} protons on target in the different τ decay channels. Since the magnet around the LDM/neutrino target has been removed in the initial revision for ECN3, ν_τ and $\overline{\nu}_\tau$ can only be distinguished in the muonic mode. For this reason, the total numbers of $\nu_\tau + \overline{\nu}_\tau$ are given for the other modes.

including the contribution from cascade production in the target. The number of charged-current deep inelastic scattering (CC DIS) interactions in the neutrino target is evaluated by convoluting the generated neutrino spectrum with the cross-section provided by the GENIE [172] Monte Carlo generator. The expected number of CC DIS in the target of the SND detector in the CDS design is reported in the first column of Table 3.

By combining the overall neutrino CC DIS interaction yield in the target with the detection efficiencies, it is possible to estimate the expected number of ν_τ and $\overline{\nu}_\tau$ interactions observed in the different decay channels. An unprecedented sample of about 20 000 ν_τ and $\overline{\nu}_\tau$ detected interactions is expected for 2×10^{20} protons on target, as reported in Table 4.

With 2×10^{20} protons on target, more than $\sim 2 \times 10^5$ neutrino-induced charmed hadrons are expected, as reported in the second column of Table 3. The total charm yield exceeds the samples available in previous experiments by more than one order of magnitude. No charm candidate from electron neutrino interactions was ever reported by any previous experiment. Consequently, all the studies on charm physics performed with neutrino interactions will be improved, and some channels inaccessible in the past will be explored. This includes the double charm production cross-section [182,183] and the search for pentaquarks with charm quark content [184]. Charmed hadrons produced in neutrino interactions are also important to investigate the strange-quark content of the nucleon. The samples available at SHiP will further allow to significantly constrain the ν_τ magnetic moment and test lepton flavour violation in the neutrino sector.

5 Expected challenges and road map

The work packages for the BDF and the SHiP Technical Design Report (TDR) studies, including the associated resource requirements, were discussed in the CDS reports [2,3]. The work packages are built on the understanding of the designs developed in the extensive joint studies performed during the six years of the Technical Proposal and CDS phases, which concentrated a large part of the effort on tuning the design of the components to maximise the signal acceptance and minimise the background. All critical components of the facility have been studied, analysed and in some cases prototyped. The target system has been through a first validation in a beam test in which the operating conditions of the real target

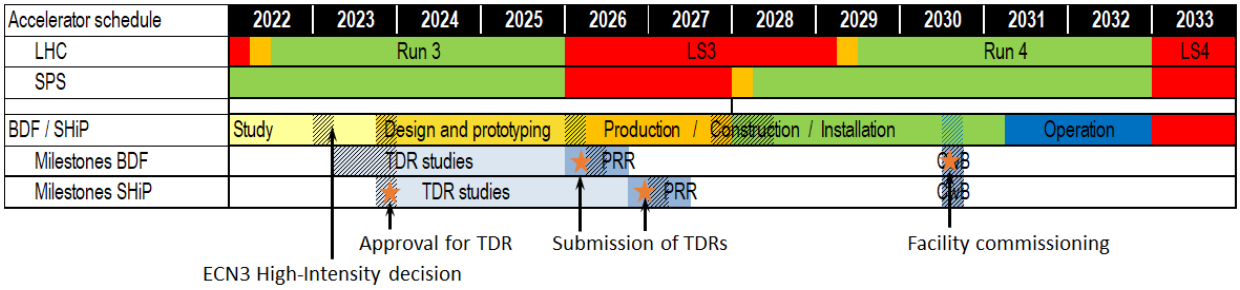

Figure 10: Implementation timeline for BDF/SHiP in ECN3.

were reproduced [16,19]. All the SHiP sub-detectors have undergone at least a first level of prototyping, and measurements with the prototypes in test beam [2,46]. In particular, the MRPC technology for the UBT, the liquid scintillator technology for the SBT, and the scintillating bar technology for the timing detector have had larger-scale prototypes in test beam. The beam tests have revealed the main technological challenges to be addressed during the TDR phase. With this information at hand, all major subsystems of the SHiP detector have been through conceptual design reviews, with the focus on outlining the work up to TDR. The SND@LHC experiment [180] currently installed and operating in TI18 of the LHC is an outstanding demonstration of the detector concept first developed for the OPERA experiment, and then improved within SHiP. Collaboration with SND@LHC is established to pursue the development of the SND detector for BDF/SHiP, and most importantly, the studies towards an upgraded SND@LHC can make significant contributions to the LDM/neutrino programme at BDF/SHiP.

For BDF, the main challenges are associated with the implementation of the target system and its cooling, and the design and handling of the target complex. Further reduction of the residual dose rate as well as decay heat could be achieved through the development of niobium-alloy cladding. Three options with helium, nitrogen, or alternatively vacuum have been considered for the vessel that should ensure an inert atmosphere to prevent corrosion and reduce residual gas radio-activation within the target shielding. These need detailed investigations, together with the design of the proximity shielding and services. While the concepts around the handling of the target and the target complex are well developed, the different components involved and the remote handling techniques also require detailed design and prototyping.

The principal technological challenges for the experiment lie in the further development of the muon shield, the decay volume and the spectrometer magnets, and involve mechanics and the full-size production. It is essential to explore various superconducting options for the muon shield with the potential to enhance the physics reach, and for the spectrometer magnets with the aim to reduce the power consumption and the operational costs. The integration of the SBT and the HSDS spectrometer tracker is associated with important design challenges that must be addressed early in the TDR phase.

The implementation of BDF/SHiP at ECN3 primarily amounts to a re-optimisation of the facility and the detector. The main implication is in the approach to the assembly and installation of the experiment without the top access that was foreseen in the CDS design [3].

The implementation timeline for BDF/SHiP in ECN3, shown in Fig. 10, draws on the

experience from the CDS phase, and has been drawn up to make maximum use of the SPS in parallel to the HL-LHC. At the same time, it aims at respecting the technical and resource constraints, and the operating schedule of the CERN beam facilities during the construction. The timeline assumes that the decision to proceed with the high-intensity upgrade of the beam line to ECN3 is taken in the first half of 2023 and that the project is approved for TDR by beginning 2024. With the three years CDS study and work under the MoU for the continued BDF R&D 2021-2023, Technical Design Reports could be delivered within two and half years for the BDF components in TCC8 and ECN3, and within three years for the SHiP detector. This is compatible with commencing the implementation of BDF/SHiP during LS3.

The LS3 for the injectors, currently scheduled 2026-2027, is a critical ingredient in the timeline since it would allow carrying out the work in the beam lines for the upgraded intensity, including the necessary cool-down, before the North Area is expected to be operational for Run 4. It is assumed that decommissioning of the current installations in TCC8 and ECN3 can be done during 2026 and 2027 such that the modifications to the infrastructure can start by the second half of 2027. It is estimated that the detector production will require three years, and that the detector assembly and installation will require two to three years. The schedule aims at a short commissioning run in the second half of 2030 with a fully operational target complex and muon shield, and operation with a complete detector in 2031.

5.1 Status of the Collaboration

SHiP is currently a collaboration of 33 institutes and 5 associated institutes, in total representing 15 countries, and CERN. The formal organisation of SHiP consists of a Collaboration Board (CB), elected Interim Spokesperson, Technical Coordinator and Physics Coordinator, and the group of project conveners as ratified by the CB.

5.2 Conclusion

The SPS is currently under-exploited and could provide a yield of protons to ECN3 that puts BDF/SHiP in an outstanding position world-wide to make a break-through in the range of FIP masses and couplings that is not accessible to the energy and precision frontier experiments. ECN3 makes it possible to implement BDF at a fraction of the original cost without compromising on the physics scope and the physics reach. SHiP has demonstrated the feasibility to construct a large-scale, versatile detector capable of coping with 4×10^{19} protons per year at 400 GeV/c and ensure an extremely low background environment. With the feasibility of the facility and the detector proven, the BDF WG and the SHiP collaboration are ready to proceed with the TDR studies and commence implementation in CERN's Long Shutdown 3.

References

Reports submitted to SPSC and ESPPU2020

[1] O. Aberle, C. Ahdida, P. Arrutia, K. Balazs, J. Bernhard, M. Brugger, M. Calviani, Y. Dutheil, R.F. Ximenes, M. Fraser, F. Galleazzi, S. Gilardoni, J.-L. Grenard, T. Griesemer, R. Jacobsson, V. Kain, D. Lafarge, S. Marsh, J.M. Martin Ruiz, R.F.M. Andrade, Y. Muttoni, A. Navascues Cornago, P. Ninin, J. Osborne, R. Ramjiawan, P. Santos Diaz, F. Sanchez Galan, H. Vincke and P. Vojtyla, *Study of alternative locations for the SPS Beam Dump Facility*, Tech. Rep. CERN-SPSC-2022-009, SPSC-SR-305, CERN, Geneva (2022).

[2] SHiP collaboration, *SHiP Experiment - Comprehensive Design Study report*, Tech. Rep. CERN-SPSC-2019-049, SPSC-SR-263, CERN, Geneva (Dec, 2019).

[3] C. Ahdida et al., *SPS Beam Dump Facility - Comprehensive Design Study*, CERN Yellow Reports: Monographs, CERN, Geneva (Dec, 2019), 10.23731/CYRM-2020-002, [1912.06356].

[4] SHiP collaboration, *SHiP Experiment - Progress Report*, Tech. Rep. CERN-SPSC-2019-010, SPSC-SR-248, CERN, Geneva (Jan, 2019).

[5] C. Ahdida et al., *SPS Beam Dump Facility - Comprehensive overview*, submitted to EPPSU, 2018.

[6] SHiP collaboration, C. Ahdida et al., *The SHiP experiment at the SPS Beam Dump Facility - Comprehensive overview*, submitted to EPPSU, 2018.

[7] I. Bezshyiko et al., *TauFV: a fixed-target experiment to search for flavour violation in tau decays*, submitted to EPPSU, 2018.

[8] SHiP collaboration, *Measurement of associated charm production induced by 400 GeV/c protons - proposal*, Tech. Rep. CERN-SPSC-2017-033. SPSC-EOI-017, CERN, Geneva (Oct, 2017).

[9] SHiP collaboration, *Muon flux measurements for SHiP at H4 - proposal*, Tech. Rep. CERN-SPSC-2017-020. SPSC-EOI-016, CERN, Geneva Jun 2017.

[10] SHiP collaboration, *A Facility to Search for Hidden Particles (SHiP) at the CERN SPS (Addendum to Technical Proposal)*, Tech. Rep. CERN-SPSC-2015-040, SPSC-P-350-ADD-2, CERN, Geneva (Oct, 2015).

[11] M. Anelli et al., *A Facility to Search for Hidden Particles (SHiP) at the CERN SPS - the SHiP physics case*, Tech. Rep. CERN-SPSC-2015-017, SPSC-P-350-ADD-1, SPSC-P-350-ADD-1, [1504.04855], CERN, Geneva (Apr, 2015).

[12] SHiP collaboration, *A Facility to Search for Hidden Particles (SHiP) at the CERN SPS - Technical Proposal*, Tech. Rep. CERN-SPSC-2015-016, SPSC-P-350, SPSC-P-350, [1504.04956], CERN, Geneva (Apr, 2015).

[13] G. Arduini, M. Calviani, K. Cornelis, L. Gatignon, B. Goddard, A. Golutvin, R. Jacobsson, J. Osborne, S. Roesler, T. Ruf, H. Vincke and H. Vincke, *A new Experiment to Search for Hidden Particles (SHIP) at the SPS North Area*, Tech. Rep. EDMS 1369559, EN-DH-2014-007 (July, 2014).

[14] W. Bonivento, A. Boyarsky, H. Dijkstra, U. Egede, M. Ferro-Luzzi, B. Goddard, A. Golutvin, D. Gorbunov, R. Jacobsson, J. Panman, M. Patel, O. Ruchayskiy, T. Ruf, N. Serra, M. Shaposhnikov and D. Treille, *Proposal to Search for Heavy Neutral Leptons at the SPS*, Tech. Rep. CERN-SPSC-2013-024, SPSC-EOI-010, SPSC-EOI-010 [1310.1762], CERN, Geneva (Oct, 2013).

Reports on the facility developments

[15] P.A. Arrutia Sota, P.N. Burrows, M.A. Fraser and F.M. Velotti, *Millisecond burst extractions from synchrotrons using RF phase displacement acceleration*, *Nucl. Instrum. Meth. A* **1039** (2022) 167007.

[16] R.F. Ximenes, O. Aberle, C. Ahdida, P. Avigni, M. Battistin, L. Bianchi, L. Buonocore, S. Burger, J. Busom, M. Calviani, J.C. Espadanal, M. Casolino, M.D. Castro, M. Fraser, S. Gilardoni, S. Girod, J. Grenard, D. Grenier, M. Guinchard, R. Jacobsson, M. Lamont, E.L. Sola, A.O. Rolo, A. Perillo-Marcone, Y. Pira, B. Riffaud, V. Vlachoudis and L. Zuccalli, *CERN BDF Prototype Target Operation, Removal and Autopsy Steps*, in *Proc. IPAC'21, Campinas, SP, Brazil*, no. 12 in International Particle Accelerator Conference, pp. 3559–3562, JACoW Publishing, Geneva, Switzerland, 08, 2021, DOI.

[17] M. Pari, F.M. Velotti, M.A. Fraser, V. Kain and O. Michels, *Characterization of the slow extraction frequency response*, *Phys. Rev. Accel. Beams* **24** (2021) 083501.

[18] B. Goddard, B. Balhan, J. Borburgh, L. Esposito, M.A. Fraser, L. Jorat, V. Kain, C. Lolliot, L.S. Stoel, P. van Trappen, F.M. Velotti, D. Barna and D. Veres, *Reduction of 400* GeV/*c slow extraction beam loss with a wire diffuser at the cern super proton synchrotron*, *Phys. Rev. Accel. Beams* **23** (2020) 023501.

[19] E. Lopez Sola, M. Calviani, O. Aberle, C. Ahdida, P. Avigni, M. Battistin, L. Bianchi, S. Burger, J. Busom Descarrega, J. Canhoto Espadanal, E. Cano-Pleite, M. Casolino, M.A. Fraser, S. Gilardoni, S. Girod, J.-L. Grenard, D. Grenier, M. Guinchard, C. Hessler, R. Jacobsson, M. Lamont, A. Ortega Rolo, M. Pandey, A. Perillo-Marcone, B. Riffaud, V. Vlachoudis and L. Zuccalli, *Beam impact tests of a prototype target for the Beam Dump Facility at CERN: Experimental setup and preliminary analysis of the online results*, *Phys. Rev. Accel. Beams* **22** (2019) 123001.

[20] C. Ahdida, M. Casolino, F. Malacrida, H. Vincke and P. Vojtyla, *Radiological Assessment of the Beam Dump Facility at CERN*, Tech. Rep. EDMS 2263868 (Dec, 2019).

[21] P. Avigni and M. Battistin and M. Calviani and P. Dalakov and K. Kershaw and J. Klier and M. Lamont and E. Lopez Sola and J.M. Martin Ruiz, *Design of a helium passivation system for the target vessel of the beam dump facility at CERN*, *JINST* **14** (2019) T12001.

[22] E. Lopez Sola, M. Calviani, P. Avigni, M. Battistin, J. Busom Descarrega, J. Canhoto Espadanal, M.A. Fraser, S. Gilardoni, B. Goddard, D. Grenier, R. Jacobsson, K. Kershaw, M. Lamont, A. Perillo-Marcone, M. Pandey, B. Riffaud, S. Sgobba, V. Vlachoudis and L. Zuccalli, *Design of a high power production target for the Beam Dump Facility at CERN*, *Phys. Rev. Accel. Beams* **22** (2019) 113001.

[23] M.A. Fraser, B. Goddard, V. Kain, M. Pari, F.M. Velotti, L.S. Stoel and M. Benedikt, *Demonstration of slow extraction loss reduction with the application of octupoles at the CERN Super Proton Synchrotron*, *Phys. Rev. Accel. Beams* **22** (2019) 123501.

[24] V. Kain, F.M. Velotti, M.A. Fraser, B. Goddard, J. Prieto, L.S. Stoel and M. Pari, *Resonant slow extraction with constant optics for improved separatrix control at the extraction septum*, *Phys. Rev. Accel. Beams* **22** (2019) 101001.

[25] F.M. Velotti, L.S. Esposito, M.A. Fraser, V. Kain, S. Gilardoni, B. Goddard, M. Pari, J. Prieto, R. Rossi, W. Scandale, L.S. Stoel, F. Galluccio, M. Garattini and Y. Gavrikov, *Septum shadowing by means of a bent crystal to reduce slow extraction beam loss*, *Phys. Rev. Accel. Beams* **22** (2019) 093502.

[26] F. Velotti, M. Fraser, B. Goddard, V. Kain and L. Stoel, *Tracking Simulations of Shadowing Electrostatic Septum Wires by Means of Bent Crystals*, in *Proc. 10th International Particle Accelerator Conference (IPAC'19), Melbourne, Australia, 19-24 May 2019*, no. 10 in International Particle Accelerator Conference, (Geneva, Switzerland), pp. 2395–2398, JACoW Publishing, Jun., 2019, DOI.

[27] F. Velotti et al., *Demonstration of Loss Reduction Using a Thin Bent Crystal to Shadow an Electrostatic Septum During Resonant Slow Extraction*, in *Proc. 10th International Particle Accelerator Conference (IPAC'19), Melbourne, Australia, 19-24 May 2019*, no. 10 in International Particle Accelerator Conference, (Geneva, Switzerland), pp. 3399–3403, JACoW Publishing, Jun., 2019, DOI.

[28] Y. Dutheil et al., *Update on Beam Transfer Line Design for the SPS Beam Dump Facility*, in *Proc. 10th International Particle Accelerator Conference (IPAC'19), Melbourne, Australia, 19-24 May 2019*, no. 10 in International Particle Accelerator Conference, (Geneva, Switzerland), pp. 2375–2378, JACoW Publishing, Jun., 2019, DOI.

[29] SHiP collaboration, *The experimental facility for the Search for Hidden Particles at the CERN SPS*, *JINST* **14** (2019) P03025.

[30] B. Balhan, P. Bestmann, D. Bjorkman, J. Borburgh, M. Butcher, M. Calviani, M. Di Castro, M. Donze, L.S. Esposito, M.A. Fraser, F. Galluccio, Y. Gavrikov, S. Gilardoni, B. Goddard, L.O. Jorat, A. Harrison, S. Hirlander, R. Jacobsson, V. Kain, I. Lamas Garcia, J. Lendaro, A. Masi, D. Mirarchi, M. Pari, J. Prieto Prieto, S. Redaelli, R. Rossi, W. Scandale, R. Seidenbinder, P. Serrano Galvez, L. Stoel, F.M. Velotti and C. Zamantzas, *Improvements to the SPS Slow Extraction for High Intensity Operation*, Tech. Rep. CERN-ACC-NOTE-2019-0010, CERN-PBC-Notes-2021-007 (Mar, 2019).

[31] C. Heßler, M. Calviani, Y. Dutheil, M. Fraser, B. Goddard, V. Kain, E.L. Sola, F. Velotti et al., *Beam Optics Studies for BDF and for Tests of a Prototype Target*, in *9th Int. Particle Accelerator Conf.(IPAC'18), Vancouver, BC, Canada, April 29-May 4, 2018*, pp. 754–757, JACOW Publishing, Geneva, Switzerland, 2018.

[32] H. Bartosik, G. Arduini, M.A. Fraser, L. Gatignon, B. Goddard, R. Jacobsson, V. Kain and E. Koukovini Platia, *SPS Operation and Future Proton Sharing scenarios for the SHiP experiment at the BDF facility*, Tech. Rep. CERN-ACC-NOTE-2018-0082, CERN-PBC-Notes-2021-008 (Dec, 2018).

[33] Y. Dutheil, J. Bauche, M. Calviani, L. Dougherty, M. Fraser, B. Goddard, C. Heßler, J. Kurdej and E.L. Sola, *Beam transfer line design to the SPS Beam Dump Facility*, in *Proc. 9th International Particle Accelerator Conference (IPAC'18), Vancouver, BC, Canada*, pp. 751–753, 2018.

[34] K. Kershaw, J.-L. Grenard, M. Calviani, C. Ahdida, M. Casolino, S. Delavalle, D. Hounsome, R. Jacobsson, M. Lamont, E.L. Sola, R. Scott, V. Vlachoudis and H. Vincke, *Design Development for the Beam Dump Facility Target Complex at CERN*, *JINST* **13** (2018) P10011.

[35] F. Addesa et al., *The SE-CpFM Detector for the Crystal-Assisted Extraction at CERN-SPS*, in *Proc. of International Beam Instrumentation Conference (IBIC'17), Grand Rapids, MI, USA, 20-24 August 2017*, no. 6 in International Beam Instrumentation Conference, (Geneva, Switzerland), pp. 419–422, JACoW, Mar, 2018, http://jacow.org/ibic2017/papers/wepcf04.pdf.

[36] J.A. Osborne and M. Manfredi, *Civil Engineering for the SHiP facility*, Tech. Rep. CERN-SHiP-NOTE-2015-008, EDMS 1499253 (Mar, 2015).

[37] C.C. Strabel, H. Vincke and H. Vincke, *Radiation protection studies for the SHiP facility*, Tech. Rep. CERN-SHiP-NOTE-2015-007, EDMS 1490910 (Apr, 2015).

[38] M. Calviani, M. Battistin, R. Betemps, J.-L. Grenard, D. Horvath, A. Perillo Marcone, A.J. Rakai, R. Rinaldesi, S. Sgobba, C.C. Strabel, V. Venturi, H. Vincke, A.P. Perez and A. Pacholek, *Conceptual design of the SHiP Target and Target Complex*, Tech. Rep. CERN-SHiP-NOTE-2015-006, EDMS 1465053 (Apr, 2015).

[39] B. Goddard, M.A. Fraser, J. Borburgh, B. Balhan, G. Le Godec, M. Zerlauth, D. Tommasini, V. Kain, K. Cornelis, J. Wenninger, L. Jensen, B. Todd, J. Bauche and B. Puccio, *Extraction and beam transfer for the SHiP facility*, Tech. Rep. CERN-SHiP-NOTE-2015-005, EDMS 1495859 (Apr, 2015).

[40] G. Arduini, B. Goddard, L. Gatignon and K. Cornelis, *The SPS beam parameters, the operational cycle, and proton sharing with the SHiP facility*, Tech. Rep. CERN-SHiP-NOTE-2015-004, EDMS 1498984 (Mar, 2015).

Reports on the detector developments

[41] M. Koratzinos and E. Van Herwijnen, *A possible yokeless superconducting dipole for the SHiP muon shield*, Tech. Rep. CERN-SHiP-INT-006 (2022).

[42] M. Ferro-Luzzi, *Preliminary exploration of a superconducting muon shield*, Tech. Rep. CERN-SHiP-INT-2022-005 (2022).

[43] P. Wertelaers, *Normal-conducting muon shield with standard yoke iron and tuned return yoke ; first performance assessment*, Tech. Rep. CERN-SHiP-INT-2022-004 (2022).

[44] P. Wertelaers, *Muon shield concept based on superconducting magnet and tuned iron return yoke*, Tech. Rep. CERN-SHiP-INT-2022-003 (2022).

[45] P. Wertelaers, *Deterministic trace computation of charged particle in three dimensions*, Tech. Rep. CERN-SHiP-INT-2022-002 (2022).

[46] S. Collaboration, *The SHiP experiment at the proposed CERN SPS Beam Dump Facility*, *Eur. Phys. J. C* **82** (2022) 486.

[47] SHiP collaboration, *Track reconstruction and matching between emulsion and silicon pixel detectors for the SHiP-charm experiment*, *JINST* **17** (2022) P03013 [2112.11754].

[48] SHiP SBT Collaboration collaboration, *First measurement of the surface tension of a liquid scintillator based on Linear Alkylbenzene (HYBLENE 113)*, *JINST* **17** (2022) T05012. 5 p [2201.12139].

[49] A. Miano, A. Fiorillo, A. Salzano, A. Prota and R. Jacobsson, *The structural design of the decay volume for the Search for Hidden Particles (SHIP) project*, *Archives of Civil and Mechanical Engineering* **21** (2021) 3.

[50] SHIP collaboration, *The BIM-based Integrated Design of the SHiP Project Decay Volume*, *IOP Conf. Ser. Mater. Sci. Eng.* **1044** (2021) 012009.

[51] SHiP collaboration, *Reconstruction of 400 GeV/c proton interactions with the SHiP-charm project*, Tech. Rep. CERN-SHiP-NOTE-2020-002 (Nov, 2020).

[52] H. Bajas and D. Tommasini, *SHiP spectrometer magnet – Superconducting options*, Tech. Rep. CERN-SHiP-NOTE-2022-001 (EDMS 2440157) (Apr, 2020).

[53] SHiP collaboration, *A prototype for the SHiP timing detector*, *Nucl. Instrum. Meth. A* **979** (2020) 164398.

[54] SHiP collaboration, *A timing detector for the SHiP experiment*, *Nucl. Instrum. Meth.* **A924** (2019) 369.

[55] D. Sukhonos and A. Zelenov, *Spectrometer Straw Tracker 2017 Test Beam Results*, Tech. Rep. CERN-SHiP-INT-2019-005 (Dec, 2019).

[56] D. Bick, S. Bieschke, C. Hagner, B. Kaiser and W. Schmidt-Parzefall, *The Suspended Bridge Design Concept for the SHiP Spectrometer Straw Tracker*, Tech. Rep. CERN-SHiP-INT-2019-006 (Dec, 2019).

[57] P. Wertelaers, *Expanding piano frame for Straw Tracker*, Tech. Rep. CERN-SHiP-INT-2019-007 (Dec, 2019).

[58] P. Wertelaers et al., *SHiP Hidden Sector spectrometer magnet*, Tech. Rep. CERN-SHiP-INT-2019-008 (Dec, 2019).

[59] P. Wertelaers et al., *SHiP Hidden Sector detector vacuum system*, Tech. Rep. CERN-SHiP-INT-2019-010 (Dec, 2019).

[60] P. Wertelaers et al., *SHiP Hidden Sector spectrometer vacuum tank*, Tech. Rep. CERN-SHiP-INT-2019-009 (Dec, 2019).

[61] SHiP collaboration, *Development of a magnet system for the CERN BDF/SHiP Facility*, Tech. Rep. CERN-SHiP-NOTE-2019-004 (Oct, 2019).

[62] E. Graverini, *The detectors of the SHiP experiment at CERN – Proceedings of Frontier Detectors for Frontier Physics: 14th Pisa Meeting on Advanced Detectors*, *Nucl. Instrum. Meth. A* **936** (2019) 724.

[63] M. Ehlert, A. Hollnagel, I. Korol, A. Korzenev, H. Lacker, P. Mermod, J. Schliwinski, L. Shihora, P. Venkova and M. Wurm, *Proof-of-principle measurements with a liquid-scintillator detector using wavelength-shifting optical modules*, *Journal of Instrumentation* **14** (2019) P03021.

[64] SHiP collaboration, *SHiP Hidden Sector Muon System: Progress report.*, Tech. Rep. CERN-SHiP-NOTE-2019-002 (Nov, 2019).

[65] G. De Lellis, *The SHiP experiment and the RPC technology*, *Journal of Instrumentation* **14** (2019) C06009.

[66] SHiP collaboration, *The Magnet of the Scattering and Neutrino Detector for the SHiP experiment at CERN*, 1910.02952.

[67] A. Alexandrov, G. De Lellis and V. Tioukov, *A Novel Optical Scanning Technique with an Inclined Focusing Plane*, *Sci. Rep.* **9** (2019) 2870.

[68] P. Santos Diaz, *Preliminary design of the decay volume vacuum system for the SHiP experiment*, Tech. Rep. CERN EDMS 2000025 Jan 2019.

[69] SHiP collaboration, *The CERN-2017 engineering design concept of a generic straw station for the Spectrometer Tracker*, Tech. Rep. CERN-SHiP-INT-2018-001 (Dec, 2018).

[70] SHiP collaboration, *Studies for the electro-magnetic calorimeter SplitCal for the SHiP experiment at CERN with shower direction reconstruction capability*, *JINST* **13** (2018) C02041.

[71] SHiP collaboration, *The active muon shield in the SHiP experiment*, *JINST* **12** (2017) P05011 [1703.03612].

[72] SHiP collaboration, *Optimising the active muon shield for the SHiP experiment at CERN*, *J. Phys. Conf. Ser.* **934** (2017) 012050.

[73] C. Betancourt et al., *Application of large area SiPMs for the readout of a plastic scintillator based timing detector*, *JINST* **12** (2017) P11023 [1709.08972].

[74] B. Hosseini and W.M. Bonivento, *Particle Identification tools and performance in the SHiP Experiment*, Tech. Rep. CERN-SHiP-NOTE-2017-002 Jul 2017.

[75] W. Baldini, A. Blondel, A. Calcaterra, R. Jacobsson, A. Khotjantsev, Y. Kudenko, V. Kurochka, G. Lanfranchi, A. Mefodiev, O. Mineev, A. Montanari, E.N. Messomo, A. Saputi and N. Tosi, *Measurement of parameters of scintillating bars with wavelength-shifting fibres and silicon photomultiplier readout for the SHiP muon detector*, *Journal of Instrumentation* **12** (2017) P03005.

[76] SHiP collaboration, *Simulation and pattern recognition for the SHiP Spectrometer Tracker*, Tech. Rep. CERN-SHiP-NOTE-2015-002 Mar 2015.

Reports on physics studies

[77] M. Ferro-Luzzi, *How the distance of the cavern walls affects the background rates*, Tech. Rep. CERN-SHiP-INT-2022-001 (Jan, 2022).

[78] SHiP collaboration, *Sensitivity of the SHiP experiment to light dark matter*, *JHEP* **04** (2021) 199 [2010.11057].

[79] SHiP collaboration, *Sensitivity of the SHiP experiment to dark photons decaying to a pair of charged particles*, *Eur. Phys. J. C* **81** (2021) 451 [2011.05115].

[80] SHiP collaboration, *Measurement of the muon flux from 400 GeV/c protons interacting in a thick molybdenum/tungsten target*, *Eur. Phys. J. C* **80** (2020) 284.

[81] SHiP collaboration, *Sensitivity of the SHiP experiment to Heavy Neutral Leptons*, *JHEP* **04** (2019) 077 [1811.00930].

[82] D. Sukhonos, M. Ferro-Luzzi and T. Ruf, *Hit Rates in the Spectrometer Straw Tracker from Simulation*, Tech. Rep. CERN-SHiP-INT-2019-002 (Jun, 2019).

[83] SHiP collaboration, *Fast simulation of muons produced at the SHiP experiment using Generative Adversarial Networks*, *JINST* **14** (2019) P11028 [1909.04451].

[84] M. De Serio, *Neutrino physics with the SHiP experiment at CERN*, *PoS* **EPS-HEP2017** (2017) 101.

[85] T. Ruf, *Studying Multiple Scattering with GEANT4 v10.3.2*, Tech. Rep. CERN-SHiP-NOTE-2017-003 Dec 2018.

[86] E. Graverini, E. Van Herwijnen and T. Ruf, *Mass dependence of branching ratios into HNL for FairShip*, Tech. Rep. CERN-SHiP-NOTE-2016-001 (2016).

[87] H. Dijkstra and T. Ruf, *Heavy Flavour Cascade Production in a Beam Dump*, Tech. Rep. CERN-SHiP-NOTE-2015-009 Dec 2015.

Reports on theory developments

[88] A.M. Abdullahi et al., *The Present and Future Status of Heavy Neutral Leptons*, in *2022 Snowmass Summer Study*, 3, 2022 [2203.08039].

[89] S. Eijima, M. Shaposhnikov and I. Timiryasov, *Freeze-in and freeze-out generation of lepton asymmetries after baryogenesis in the νMSM*, *JCAP* **04** (2022) 049 [2011.12637].

[90] Y. Borysenkova, P. Kashko, M. Tsarenkova, K. Bondarenko and V. Gorkavenko, *Production of Chern-Simons bosons in decays of mesons*, *J. Phys. G* **49** (2022) 085003 [2110.14500].

[91] K. Bondarenko, A. Boyarsky, J. Klaric, O. Mikulenko, O. Ruchayskiy, V. Syvolap and I. Timiryasov, *An allowed window for heavy neutral leptons below the kaon mass*, *JHEP* **07** (2021) 193 [2101.09255].

[92] J. Klarić, M. Shaposhnikov and I. Timiryasov, *Reconciling resonant leptogenesis and baryogenesis via neutrino oscillations*, *Phys. Rev. D* **104** (2021) 055010 [2103.16545].

[93] J. Klarić, M. Shaposhnikov and I. Timiryasov, *Uniting Low-Scale Leptogenesis Mechanisms*, *Phys. Rev. Lett.* **127** (2021) 111802 [2008.13771].

[94] D. Gorbunov, I. Krasnov, Y. Kudenko and S. Suvorov, *Heavy Neutral Leptons from kaon decays in the SHiP experiment*, *Phys. Lett. B* **810** (2020) 135817 [2004.07974].

[95] K. Bondarenko, A. Boyarsky, T. Bringmann, M. Hufnagel, K. Schmidt-Hoberg and A. Sokolenko, *Direct detection and complementary constraints for sub-GeV dark matter*, *JHEP* **03** (2020) 118 [1909.08632].

[96] I. Boiarska, K. Bondarenko, A. Boyarsky, V. Gorkavenko, M. Ovchynnikov and A. Sokolenko, *Phenomenology of GeV-scale scalar portal*, *JHEP* **11** (2019) 162 [1904.10447].

[97] K. Bondarenko, A. Boyarsky, M. Ovchynnikov and O. Ruchayskiy, *Sensitivity of the intensity frontier experiments for neutrino and scalar portals: analytic estimates*, *JHEP* **08** (2019) 061 [1902.06240].

[98] I. Boiarska, K. Bondarenko, A. Boyarsky, S. Eijima, M. Ovchynnikov, O. Ruchayskiy and I. Timiryasov, *Probing baryon asymmetry of the Universe at LHC and SHiP*, 1902.04535.

[99] A. Monin, A. Boyarsky and O. Ruchayskiy, *Hadronic decays of a light higgs-like scalar*, *Physical Review D* **99** (2019) .

[100] J.-L. Tastet and I. Timiryasov, *Dirac vs. Majorana HNLs (and their oscillations) at SHiP*, 1912.05520.

[101] S. Eijima, M. Shaposhnikov and I. Timiryasov, *Parameter space of baryogenesis in the νMSM*, *JHEP* **07** (2019) 077 [1808.10833].

[102] S. Demidov, S. Gninenko and D. Gorbunov, *Light hidden photon production in high energy collisions*, *JHEP* **07** (2019) 162 [1812.02719].

[103] K. Bondarenko, A. Boyarsky, D. Gorbunov and O. Ruchayskiy, *Phenomenology of GeV-scale Heavy Neutral Leptons*, *JHEP* **11** (2018) 032 [1805.08567].

[104] F. Bezrukov, D. Gorbunov and I. Timiryasov, *Uncertainties of hadronic scalar decay calculations*, 1812.08088.

[105] S. Eijima, M. Shaposhnikov and I. Timiryasov, *Freeze-out of baryon number in low-scale leptogenesis*, *JCAP* **11** (2017) 030 [1709.07834].

[106] S. Eijima and M. Shaposhnikov, *Fermion number violating effects in low scale leptogenesis*, *Phys. Lett. B* **771** (2017) 288 [1703.06085].

[107] S. Alekhin et al., *A facility to search for hidden particles at the CERN SPS: the SHiP physics case*, *Reports on Progress in Physics* **79** (2016) 124201.

PhD theses

[108] P. Arrutia Sota, *Beam delivery studies for future slow extracted beams at CERN (Preliminary)*, **Expected 2024**.

[109] O. Mikulenko, *Reconstructing the properties of new particle with beam dump experiments (Preliminary)*, **Expected 2023**.

[110] L. Congedo, *Development of new generation gas detectors and readout system for muon identification in the SHiP experiment(Preliminary)*, **Expected Feb 2023**.

[111] N. Owtscharenko, *Development and operation of a silicon pixel tracker for the SHiP-charm experiment (Preliminary)*, **Expected Jan 2023**.

[112] I. Boiarska, *Chasing feebly interacting particles*, Sep 2022. https://nbi.ku.dk/english/Calendar/activities_22/phd-defense-by-iryna-boiarska/.

[113] M. Ovchynnikov, *Searches for new physics in the laboratory and in space*, 2021. https://www.prophy.science/article/155910750-Searches-for-new-physics-in-the-laboratory-and-in-space/.

[114] J.-L. Tastet, *Searching for Heavy Neutral Leptons at CERN*, 2021. https://www.prophy.science/article/155911516-Searching-for-Heavy-Neutral-Leptons-at-CERN/.

[115] S. Shirobokov, *Optimisation of the SHiP Beam Dump Facility with generative surrogate models*, 2021. https://spiral.imperial.ac.uk/handle/10044/1/95975.

[116] A. Marshall, *Machine learning based background simulations and R-parity violating neutralinos at SHiP and contributions to the angular analysis of* $B^0 \to K^{*0} (\to K^+\pi^-)\, \mu^+\mu^-$ *at LHCb*, 2021. https://cds.cern.ch/record/2792495.

[117] P. Chau, *Optimierung von hochauflösenden Sampling-Kalorimetern mit szintillatorbasierter SiPM-Auslese (Optimization of high-resolution sampling calorimeters with scintillator-based SiPM-readout)*, 2021. https://openscience.ub.uni-mainz.de/handle/20.500.12030/7057.

[118] I. Bezshyiko, *Testing the Standard Model Lepton Symmetries in Collider and Fixed-Target Experiments*, 2021. https://cds.cern.ch/record/2783225.

[119] A. Iuliano, *Event reconstruction and data analysis techniques for the SHiP experiment*, 2021. https://cds.cern.ch/record/2776128.

[120] D. Sukhonos, *Spectrometer Straw Tracker design studies for the SHiP experiment - Universitẗ Hamburg*, 2020. https://cds.cern.ch/record/2746452.

[121] S. Bieschke, *The Drift Tube Spectrometer for the Measurement of the Muon Flux and Spectrum Emerging from a Proton Beam Dump at the SPS for the SHiP Experiment - Universität Hamburg*, 2020. https://ediss.sub.uni-hamburg.de/handle/ediss/8972.

[122] O. Lantwin, *Optimisation of the SHiP experimental design*, 2019. https://cds.cern.ch/record/2693177.

[123] K. Bondarenko, *Plan B for particle physics: finding long lived particles at CERN*, 2018. https://www.prophy.science/article/63558517-Plan-B-for-particle-physics-finding-long-lived-particles-at-CERN/.

[124] E. Graverini, *Flavour physics with (semi)leptonic decays at forward spectrometers*, 2018. https://cds.cern.ch/record/2630297.

[125] F.L. Redi, *Searching for Heavy Neutral Leptons at LHCb and SHiP*, 2017. https://cds.cern.ch/record/2716229.

[126] A. Buonaura, *Study of nu-tau properties with the SHiP experiment*, 2017. https://cds.cern.ch/record/2268663.

[127] F.M. Velotti, *Higher brightness beams from the SPS for the HL-LHC era*, 2017. https://cds.cern.ch/record/2265703.

Other references

[128] T.E.S. Group, *Deliberation document on the 2020 Update of the European Strategy for Particle Physics*, Tech. Rep. CERN-ESU-014, Geneva (2020), DOI.

[129] R.K. Ellis et al., *European Strategy for Particle Physics Preparatory Group: Physics Briefing Book*, 1910.11775.

[130] R. Alemany et al., *Summary Report of Physics Beyond Colliders at CERN*, 1902.00260.

[131] J. Jaeckel, M. Lamont and C. Vallée, *The quest for new physics with the physics beyond colliders programme*, *Nat. Phys.* **16** (2020) 393.

[132] *CERN Medium Term Plan 2021 - 2025*, Tech. Rep. CERN/SPC/1141/Rev., CERN/FC/6412/Rev., CERN/3499/Rev. (September, 2020).

[133] *BDF WG mandate*, 2021. https://pbc.web.cern.ch/bdf-mandate.

[134] *Memorandum of Understanding for the collaboration on the SPS Beam Dump Facility R&D programme*, February, 2022. https://edms.cern.ch/document/2708441.

[135] *Minutes of the 237th meeting of the Research Board, held on 9 June 2021*, Tech. Rep. CERN-DG-RB-2021-505, M-237, CERN, Geneva (Jun, 2021).

[136] J. Bernhard, M. Brugger, M. Fraser, R. Jacobsson and Y. Kadi, *Memorandum - Support for Engineering Studies as input to the ECN3 Beam Delivery Task Force*, July, 2022. https://edms.cern.ch/document/2758293.

[137] G. Collaboration, *The Gaia mission*, A&A **595** (2016) A1 [1609.04153].

[138] DESI collaboration, *The DESI Experiment Part I: Science,Targeting, and Survey Design*, 1611.00036.

[139] R. Laureijs et al., *Euclid Definition Study Report*, *arXiv e-prints* (2011) arXiv:1110.3193 [1110.3193].

[140] LSST collaboration, *LSST: from Science Drivers to Reference Design and Anticipated Data Products*, *Astrophys. J.* **873** (2019) 111 [0805.2366].

[141] R. Tamai, M. Cirasuolo, J.C. González, B. Koehler and M. Tuti, *The E-ELT program status*, in *Ground-based and Airborne Telescopes VI*, H.J. Hall, R. Gilmozzi and H.K. Marshall, eds., vol. 9906 of *Society of Photo-Optical Instrumentation Engineers (SPIE) Conference Series*, p. 99060W, July, 2016, DOI.

[142] M. Clampin, C. Atkinson, L. Feinberg, W. Hayden, P. Lightsey, M. Mountain and S. Texter, *Status of the JWST Observatory Design*, in *American Astronomical Society Meeting Abstracts*, vol. 203 of *American Astronomical Society Meeting Abstracts*, p. 121.01, Dec., 2003.

[143] A. Weltman et al., *Fundamental physics with the Square Kilometre Array*, *Publ. Astron. Soc. Austral.* **37** (2020) e002 [1810.02680].

[144] S. Chakrabarti et al., *Snowmass2021 Cosmic Frontier White Paper: Observational Facilities to Study Dark Matter*, in *2022 Snowmass Summer Study*, 3, 2022 [2203.06200].

[145] Y.-Y. Mao et al., *Snowmass2021: Vera C. Rubin Observatory as a Flagship Dark Matter Experiment*, 2203.07252.

[146] D. Antypas et al., *New Horizons: Scalar and Vector Ultralight Dark Matter*, 2203.14915.

[147] DESI collaboration, *A Spectroscopic Road Map for Cosmic Frontier: DESI, DESI-II, Stage-5*, 2209.03585.

[148] D. Green et al., *Snowmass Theory Frontier: Astrophysics and Cosmology*, 2209.06854.

[149] A. Drlica-Wagner et al., *Report of the Topical Group on Cosmic Probes of Dark Matter for Snowmass 2021*, 2209.08215.

[150] R.X. Adhikari et al., *Report of the Topical Group on Cosmic Probes of Fundamental Physics for for Snowmass 2021*, 2209.11726.

[151] G. Krnjaic, *Probing Light Thermal Dark-Matter With a Higgs Portal Mediator*, *Phys. Rev. D* **94** (2016) 073009 [1512.04119].

[152] K. Bondarenko, A. Boyarsky, T. Bringmann, M. Hufnagel, K. Schmidt-Hoberg and A. Sokolenko, *Direct detection and complementary constraints for sub-GeV dark matter*, *JHEP* **03** (2020) 118 [1909.08632].

[153] FOR THE N_TOF COLLABORATION collaboration, *Design development and implementation of an irradiation station at the neutron time-of-flight facility at CERN*, *Phys. Rev. Accel. Beams* **25** (2022) 103001.

[154] N. Patronis et al., *The CERN n_TOF NEAR station for astrophysics- and application-related neutron activation measurements*, 2022. 10.48550/ARXIV.2209.04443, https://arxiv.org/abs/2209.04443.

[155] F.J. Harden, A. Bouvard, N. Charitonidis and Y. Kadi, *HiRadMat: A facility beyond the realms of materials testing*, *Journal of Physics: Conference Series* **1350** (2019) 012162.

[156] E. Shaposhnikova, G. Arduini, T. Bohl, M. Chanel, R. Garoby, S. Hancock, K. Hanke, T.P.R. Linnecar, R. Steerenberg and B. Vandorpe, *Recent intensity increase in the CERN accelerator chain – Proceedings of 21st IEEE Particle Accelerator Conference, Knoxville, TN, USA, 16 - 20 May 2005*, Tech. Rep. CERN-AB-2005-029 (2005).

[157] E. Shaposhnikova, T. Argyropoulos, T. Bohl, P. Cruikshank, B. Goddard, T. Kaltenbacher, A. Lasheen, J. Perez Espinos, J. Repond, B. Salvant and C. Vollinger, *Removing Known SPS Intensity Limitations for High Luminosity LHC Goals – Proceedings of 7th International Particle Accelerator Conference, Busan, Korea, 8 - 13 May 2016*, Tech. Rep. CERN-ACC-2016-289 (2016), DOI.

[158] *CERN Fire-Induced Radiological Integrated Assessment (FIRIA)*, 2018. https://hse.cern/content/firia.

[159] H. Vincke et al., *ALARA Rule applied to interventions at CERN*, Apr, 2017. https://edms.cern.ch/document/1751123.

[160] S. Pianese et al., *Design of the Future High Energy Beam Dump for the CERN SPS*, in *Proc. 9th International Particle Accelerator Conference (IPAC'18), Vancouver, BC, Canada, April 29-May 4, 2018*, no. 9 in International Particle Accelerator Conference, (Geneva, Switzerland), pp. 2612–2615, JACoW Publishing, June, 2018, DOI.

[161] S. Pianese, A. Perillo Marcone, F.-X. Nuiry, M. Calviani, K.A. Szczurek, G. Arnau Izquierdo, P. Avigni, S. Bonnin, J. Busom Descarrega, T. Feniet, K. Kershaw, J. Lendaro, A. Perez Fontenla, T. Schubert, S. Sgobba and T. Weißgärber, *Hot isostatic pressing assisted diffusion bonding for application to the Super Proton Synchrotron internal beam dump at CERN*, *Phys. Rev. Accel. Beams* **24** (2021) 043001.

[162] C. Ahdida et al., *New Capabilities of the FLUKA Multi-Purpose Code*, *Frontiers in Physics* **9** (2022) 788253.

[163] G. Battistoni et al., *Overview of the fluka code*, *Annals of Nuclear Energy* **82** (2015) 10.

[164] *Private communication A. Devred, G. de Lellis, R. Jacobsson*, 2021 - 2022.

[165] K. Kodama, N. Saoulidou, G. Tzanakos, B. Baller, B. Lundberg, R. Rameika, J. Song, C. Yoon, S. Chung, S. Aoki, T. Hara, C. Erickson, K. Heller, R. Schwienhorst, J. Sielaff, J. Trammell, K. Hoshino, J. Kawada, M. Komatsu, M. Miyanishi, M. Nakamura, T. Nakano, K. Narita, K. Niwa, N. Nonaka, K. Okada, O. Sato, T. Toshito, S. Miyamoto, S. Takahashi, B. Park, T. Furukawa, V. Paolone and T. Kafka, *Momentum measurement of secondary particle by multiple coulomb scattering with emulsion cloud chamber in donut experiment*, *Nuclear Instruments and Methods in Physics Research Section A: Accelerators, Spectrometers, Detectors and Associated Equipment* **574** (2007) 192.

[166] M. Al-Turany, D. Bertini, R. Karabowicz, D. Kresan, P. Malzacher, T. Stockmanns and F. Uhlig, *The fairroot framework*, *Journal of Physics: Conference Series* **396** (2012) 022001.

[167] GEANT4 collaboration, *GEANT4: A Simulation toolkit*, *Nucl. Instrum. Meth.* **A506** (2003) 250.

[168] J. Allison et al., *Geant4 developments and applications*, *IEEE Trans. on Nucl. Science* **53** (2006) 270.

[169] T. Sjöstrand, *PYTHIA 5.7 and JETSET 7.4: Physics and manual*, hep-ph/9508391.

[170] T. Sjöstrand, S. Mrenna and P.Z. Skands, *PYTHIA 6.4 Physics and Manual*, *JHEP* **05** (2006) 026 [hep-ph/0603175].

[171] T. Sjöstrand, S. Mrenna and P.Z. Skands, *A Brief Introduction to PYTHIA 8.1*, *Comput. Phys. Commun.* **178** (2008) 852 [0710.3820].

[172] C. Andreopoulos et al., *The GENIE Neutrino Monte Carlo Generator*, *Nucl. Instrum. Meth.* **A614** (2010) 87 [0905.2517].

[173] CHARM Collaboration collaboration, *A search for decays of heavy neutrinos in the mass range 0.5 - 2.8 GeV*, *Phys. Lett. B* **166** (1985) 473.

[174] J. Rauch and T. Schlüter, *GENFIT — a generic track-fitting toolkit*, .

[175] J. Beacham et al., *Physics beyond colliders at CERN: beyond the Standard Model working group report*, *Journal of Physics G: Nuclear and Particle Physics* **47** (2019) 010501 [1901.09966].

[176] L. Carloni, J. Rathsman and T. Sjöstrand, *Discerning secluded sector gauge structures*, *Journal of High Energy Physics* **2011** (2011) .

[177] L. Buonocore, C. Frugiuele, F. Maltoni, O. Mattelaer and F. Tramontano, *Event generation for beam dump experiments*, *JHEP* **05** (2019) 028 [1812.06771].

[178] D. Banerjee et al., *Dark matter search in missing energy events with NA64*, *Phys. Rev. Lett.* **123** (2019) 121801 [1906.00176].

[179] BaBar collaboration, *Search for Invisible Decays of a Dark Photon Produced in e^+e^- Collisions at BaBar*, *Phys. Rev. Lett.* **119** (2017) 131804 [1702.03327].

[180] SND@LHC collaboration, *SND@LHC: The Scattering and Neutrino Detector at the LHC*, 2210.02784.

[181] A. Boyarsky, O. Mikulenko, M. Ovchynnikov and L. Shchutska, *Searches for new physics at SND@LHC*, *Journal of High Energy Physics* **2022** (2022) .

[182] CHORUS collaboration, *Observation of one event with the characteristics of associated charm production in neutrino charged-current interactions*, *Phys. Lett.* **B539** (2002) 188.

[183] HERA-B collaboration, *Measurement of D^0, D^+, D_s^+ and D^{*+} Production in Fixed Target 920-GeV Proton-Nucleus Collisions*, *Eur. Phys. J.* **C52** (2007) 531 [0708.1443].

[184] G. De Lellis, A.M. Guler, J. Kawada, U. Kose, O. Sato and F. Tramontano, *Search for charmed pentaquarks in high energy anti-neutrino interactions*, *Nucl. Phys.* **B763** (2007) 268.

BDF Working Group[30]
O. Aberle, C. Ahdida, P. Arrutia, K. Balazs, M. Calviani, Y. Dutheil, L.S. Esposito, R. Franqueira Ximenes, M. Fraser, F. Galleazzi, S. Gilardoni, J.-L. Grenard, T. Griesemer, R. Jacobsson, V. Kain, L. Krzempek, D. Lafarge, S. Marsh, J.M. Martin Ruiz, G. Mazzola, R.F. Mena Andrade, Y. Muttoni, A. Navascues Cornago, P. Ninin, J. Osborne, R. Ramjiawan, F. Sanchez Galan, P. Santos Diaz, F. Velotti, H. Vincke, P. Vojtyla

SHiP Collaboration
R. Albanese[16,d,f], J. Alt[8], A. Alexandrov[16,d], S. Aoki[19], D. Aritunov[10], A. Bay[31], C. Betancourt[32], I. Bezshyiko[32], O. Bezshyyko[38], D. Bick[9], A. Blanco[28], M. Bogomilov[1], I. Boiarska[5], K. Bondarenko[27,38], W.M. Bonivento[15], A. Boyarsky[27,38], M. Böhles[11], D. Breton[6], A. Brignoli[7], A. Buonaura[32], S. Buontempo[16], M. Campanelli[37], D. Centanni[16], K.-Y. Choi[26], M. Climescu[11], A. Conaboy[7], L. Congedo[13,a], M. Cristinziani[12], A. Crupano[14], G.M. Dallavalle[14], N. D'Ambrosio[17], R. de Asmundis[16], P. de Bryas[31], J. De Carvalho Saraiva[28], G. De Lellis[16,c], M. de Magistris[16,c], A. De Roeck[30], M. De Serio[13,a], D. De Simone[32], P. Dergachev[i], P. Deucher[11], A. Di Crescenzo[16,30,c], H. Dijkstra[i], O. Durhan[33], E. Elikkaya[33], F. Fedotovs[37], M. Ferrillo[32], M. Ferro-Luzzi[30], R.A. Fini[13], G. Fiorillo[16,c], H. Fischer[8], P. Fonte[28], R. Fresa[16,f], T. Fukuda[20], G. Galati[13,a], L. Golinka-Bezshyyko[32,38], A. Golovatiuk[16,c], A. Golutvin[36], V. Gorkavenko[38], E. Graverini[31], C. Grewing[10], A. M. Guler[33], G.J. Haefeli[31], C. Hagner[9], J.C. Helo[2,4], E. van Herwijnen[36], A. Hollnagel[11], A. Iuliano[16,c], R. Jacobsson[30], M. Jonker[30], I. Kadenko[38], C. Kamiscioglu[34], Y.G. Kim[24], N. Kitagawa[20], K. Kodama[18], D.I. Kolev[1], M. Komatsu[20], V. Kostyukhin[12], L. Krzempek[2,30], S. Kuleshov[2,3], E. Kurbatov[i], H.M. Lacker[7], O. Lantwin[i], A. Lauria[16,c], K.S. Lee[25], K.Y. Lee[23], N. Leonardo[28], V.P. Loschiavo[16,e], L. Lopes[28], F. Lyons[8], J. Maalmi[6], A.-M. Magnan[36], A.M. Marshall[35], A. Miano[16,c], S. Mikado[21], A. Mikulenko[27], M.C. Montesi[16,c], K. Morishima[20], N. Naganawa[20], M. Nakamura[20], T. Nakano[20], S. Ogawa[22], M. Ovchynnikov[27,38], N. Owtscharenko[12], B.D. Park[23], A. Pastore[13], M. Patel[36], K. Petridis[35], A. Prota[16,c], A. Quercia[16,c], A. Rademakers[30], F. Ratnikov[i], F. Redi[30], A. Reghunath[7], H. Rokujo[20], O. Ruchayskiy[5], T. Ruf[30], P. Santos Dias[30], O. Sato[20], W. Schmidt-Parzefall[9], M. Schumann[8], N. Serra[32], M. Shaposhnikov[31], L. Shchutska[31], H. Shibuya[22], S. Simone[13,a], G. Soares[28], J.Y. Sohn[23], A. Sokolenko[38], O. Soto[2,3], S. Takahashi[19], J.L. Tastet[5], I. Timiryasov[5], V. Tioukov[16], D. Tommasini[30], D. Treille[30], R. Tsenov[1], P. Ulloa[2,4], E. Ursov[i], G. Vankova-Kirilova[1], S. Vilchinski[38], C. Visone[16,c], S. van Waasen[10], P. Wertelaers[30], M. Wurm[11], S. Xella[5], D. Yilmaz[34], C.S. Yoon[23], J. Zamora Saa[2,3]

[1] *Faculty of Physics, Sofia University, Sofia, Bulgaria*
[2] *Millenium Institute For Subatomic Physics At High-Energy Frontier - SAPHIR, Chile*
[3] *Universidad Andrés Bello (UNAB)[h], Santiago, Chile*
[4] *Universidad De La Serena (ULS)[h], La Serena, Chile*
[5] *Niels Bohr Institute, University of Copenhagen, Copenhagen, Denmark*
[6] *IJCLab, CNRS, Université Paris-Saclay, Orsay, France*
[7] *Humboldt-Universität zu Berlin, Berlin, Germany*
[8] *Physikalisches Institut, Universität Freiburg, Freiburg, Germany*
[9] *Universität Hamburg, Hamburg, Germany*

[10] *Forschungszentrum Jülich GmbH (KFA), Jülich , Germany*
[11] *Institut für Physik and PRISMA Cluster of Excellence, Johannes Gutenberg Universität Mainz, Mainz, Germany*
[12] *Universität Siegen, Siegen, Germany*
[13] *Sezione INFN di Bari, Bari, Italy*
[14] *Sezione INFN di Bologna, Bologna, Italy*
[15] *Sezione INFN di Cagliari, Cagliari, Italy*
[16] *Sezione INFN di Napoli, Napoli, Italy*
[17] *Laboratori Nazionali dell'INFN di Gran Sasso, L'Aquila, Italy*
[18] *Aichi University of Education, Kariya, Japan*
[19] *Kobe University, Kobe, Japan*
[20] *Nagoya University, Nagoya, Japan*
[21] *College of Industrial Technology, Nihon University, Narashino, Japan*
[22] *Toho University, Funabashi, Chiba, Japan*
[23] *Physics Education Department & RINS, Gyeongsang National University, Jinju, Korea*
[24] *Gwangju National University of Education[d], Gwangju, Korea*
[25] *Korea University[d], Seoul, Korea*
[26] *Sungkyunkwan University[d], Suwon-si, Gyeong Gi-do, Korea*
[27] *University of Leiden, Leiden, The Netherlands*
[28] *LIP, Laboratory of Instrumentation and Experimental Particle Physics, Portugal*
[29] *Institute of Physics, University of Belgrade, Serbia*
[30] *European Organization for Nuclear Research (CERN), Geneva, Switzerland*
[31] *École Polytechnique Fédérale de Lausanne (EPFL), Lausanne, Switzerland*
[32] *Physik-Institut, Universität Zürich, Zürich, Switzerland*
[33] *Middle East Technical University (METU), Ankara, Turkey*
[34] *Ankara University, Ankara, Turkey*
[35] *H.H. Wills Physics Laboratory, University of Bristol, Bristol, United Kingdom*
[36] *Imperial College London, London, United Kingdom*
[37] *University College London, London, United Kingdom*
[38] *Taras Shevchenko National University of Kyiv, Kyiv, Ukraine*
[a] *Università di Bari, Bari, Italy*
[b] *Università di Cagliari, Cagliari, Italy*
[c] *Università di Napoli "Federico II", Napoli, Italy*
[d] *Associated to Gyeongsang National University, Jinju, Korea*
[e] *Consorzio CREATE, Napoli, Italy*
[f] *Università della Basilicata, Potenza, Italy*
[g] *Università di Napoli Parthenope, Napoli, Italy*
[h] *Associated to SAPHIR, Chile*
[i] *Individuals who made crucial contributions to this LoI*

Following the resolution of the CERN Council, Russian groups participating in the SHiP project are not included in the author list of this document. We acknowledge the contribution of the Russian scientists, in particular A. Anokhina, E. Atkin, N. Azorskiy, A. Bagulya, A.Y. Berdnikov, Y.A. Berdnikov M. Chernyavskiy, V. Dmitrenko, A. Dolmatov, T. Enik, A. Etenko, O. Fedin, K. Filippov, G. Gavrilov, V. Giuliaeva, V. Golovt-

sov, D. Golubkov, D. Gorbunov, S. Gorbunov, M. Gorshenkov, V. Grachev, V. Grichine, N. Gruzinskii, Yu. Guz, D. Karpenkov, M. Khabibullin, E. Khalikov, A. Khotyantsev, V. Kim, N. Konovalova, I. Korol'ko, I. Krasilnikova, Y. Kudenko, P. Kurbatov, V. Kurochka, E. Kuznetsova, V. Maleev, A. Malinin, A. Mefodev, O. Mineev, S. Nasybulin, B. Obinyakov, N. Okateva, A. Petrov, D. Podgrudkov, N. Polukhina, M. Prokudin, T. Roganova, V. Samsonov, E.S. Savchenko, A. Shakin, P. Shatalov, T. Shchedrina, V. Shevchenko, A. Shustov, M. Skorokhvatov, S. Smirnov, N. Starkov, P. Teterin, S. Than Naing, S. Ulin, A. Ustyuzhanin, Z. Uteshev, L. Uvarov, K. Vlasik, A. Volkov, R. Voronkov.